~~UNCLASSIFIED~~
~~CONFIDENTIAL~~

Copy 5

RM A57J22

NACA RM A57J22

C2

CLASSIFICATION CHANGED
NACA UNCLASSIFIED
CSTAR
By authority of V.9 Nr.2 Date 6-30-71 Leon 9/16/71

RESEARCH MEMORANDUM

A WIND-TUNNEL INVESTIGATION OF SEVERAL WINGLESS MISSILE CONFIGURATIONS AT SUPERSONIC SPEEDS

By David E. Reese, Jr.

Ames Aeronautical Laboratory
Moffett Field, Calif.

CLASSIFIED DOCUMENT

NATIONAL ADVISORY COMMITTEE
FOR AERONAUTICS

WASHINGTON
February 3, 1958

~~CONFIDENTIAL~~
UNCLASSIFIED

NATIONAL ADVISORY COMMITTEE FOR AERONAUTICS

RESEARCH MEMORANDUM

A WIND-TUNNEL INVESTIGATION OF SEVERAL WINGLESS MISSILE CONFIGURATIONS AT SUPERSONIC SPEEDS

By David E. Reese, Jr.

SUMMARY

A wind-tunnel investigation of several wingless missile configurations has been made. Lift, drag, and pitching-moment coefficients were measured on a series of models at Mach numbers of 2.44 to 3.35 and on one model from 1.76 to 5.05. In order to establish a frame of reference with which to evaluate the performance of the wingless missile, results are also presented for a conventional winged, cruciform missile.

The results of this investigation indicate that for the particular center-of-gravity locations chosen, the maximum trimmed lift capabilities of the wingless configurations tested were, in general, somewhat less than those of the winged missile. It is shown that a wingless missile using flared segments of the afterportion of the body to provide both stability and control can have a lower drag in the trimmed condition than one using an extendible section of the surface of the nose for control. This lower drag is achieved with some sacrifice in maximum trimmed lift capability. A comparison between Newtonian impact theory and experiment shows that the experimental values of side-force and yawing-moment coefficients due to lateral deflection of the tail control agree well with the theory at angles of attack near zero. However, the experimental rolling-moment coefficients and the side-force and yawing-moment coefficients at the higher angles of attack do not agree with the theory. The theoretical values of pitching-moment coefficient due to deflection of the control on the conical nose were in fair agreement with the experimental results, whereas this comparison for the control behind the hemispherical nose was poor.

INTRODUCTION

In the short history of guided antiaircraft missiles, airframe design has proceeded along more or less conventional lines with relatively large wings providing the forces necessary for maneuvering flight. For the

airborne missile, the use of large wings results in a rather high drag associated with the stowage of the missile and a corresponding penalty in the performance of the missile-carrying aircraft. The advantage of a reduction in the size of the missile wings, from the standpoint of minimizing this stowage drag, is obvious. Furthermore, if the wings could be eliminated entirely and folding control and stabilizing surfaces used, the additional advantage of stowing and launching the missile from a tube would be possible. This arrangement would not only have a relatively low stowage drag but should also reduce launching errors.

It can be seen then that from the standpoint of missile-airplane compatability some attention should be given to missiles having very low aspect ratio wings or no wings at all. Experimental investigations of several cruciform very low aspect ratio wing-fuselage combinations have been made by Katzen and Jorgensen (refs. 1 and 2). Experimental studies of two wingless missile configurations have been made by Lazzeroni (ref. 3) and Eggers and Syvertson (ref. 4). The present investigation was intended to explore other wingless configurations that appeared feasible from a study of these data.

The investigation reported herein was divided into three parts. The first part dealt with tests at Mach numbers of 2.44 and 3.35 of several wingless configurations utilizing a control surface located near or on the nose of the model and various types of stabilizing surfaces at the rear of the body. The second part covered the investigation at a Mach number of 3.35 of a wingless model using flared segments at the rear of the body for both stability and control. In this part of the investigation a systematic variation of the geometry of the flared segments was made, and the effects of these variations in geometry on the stability and the maximum trimmed lift and drag were determined. The third phase of the investigation covered tests made to determine the effects of Mach number on the stability, drag, and maximum trimmed lift capabilities of a model with flared body segments chosen on the basis of results obtained in the second part of the investigation. This model was tested over a Mach number range from 1.76 to 5.05. Lift, drag, and pitching-moment coefficients were obtained for all models. Side-force, yawing-moment, and rolling-moment coefficients were also obtained for the model in the third phase of the investigation at a Mach number of 2.00.

SYMBOLS

c stabilizing segment length, percent body length

c.g. center of gravity

C_D drag coefficient, $\frac{\text{drag}}{qS}$

C_{D_o} minimum drag coefficient

C_{D_T} drag coefficient at maximum trimmed lift

C_l rolling-moment coefficient, $\frac{\text{rolling moment}}{qSd}$

C_L lift coefficient, $\frac{\text{lift}}{qS}$

C_{L_T} maximum trimmed lift coefficient

C_m pitching-moment coefficient, $\frac{\text{pitching moment}}{qSd}$

ΔC_m pitching-moment coefficient at $\alpha = 0^\circ$

C_{m_α} pitching-moment-curve slope, per deg

C_n yawing-moment coefficient, $\frac{\text{yawing moment}}{qSd}$

C_Y side-force coefficient, $\frac{\text{side force}}{qS}$

d body diameter, in.

l body length, in.

M free-stream Mach number

q free-stream dynamic pressure, lb/sq in.

R Reynolds number based on body length

S maximum cross-sectional area of body, sq in.

α angle of attack of body axis, deg

δ control deflection, deg

δ_f initial flare angle of stabilizing segments, deg

φ roll angle, deg

APPARATUS

Wind Tunnels

The portions of the experimental investigation made at Mach numbers of 2.44 and 3.35 were conducted in the Ames 1- by 3-foot supersonic wind tunnel No. 2 which is an intermittent-operation, nonreturn, variable-

pressure wind tunnel with a maximum Mach number of 3.8. The Mach number in this tunnel is varied by means of flexible plates forming the top and bottom of the nozzle section. The tests at Mach numbers of 1.76, 2.0, and 2.2 were conducted in the Ames 6- by 6-foot supersonic wind tunnel. This wind tunnel is equipped with an asymmetric nozzle enabling continuous variation of Mach number up to a maximum value of 2.3. The stagnation pressure can be regulated to maintain a fixed Reynolds number. The tests at Mach numbers of 3.0, 4.24, and 5.05 were made in the Ames 10- by 14-inch hypersonic wind tunnel which is of the continuous-flow, nonreturn type and operates with a nominal supply pressure of 6 atmospheres. The Mach number in the test section may be varied from approximately 2.7 to 6.3 by changing the relative position of the top and bottom walls of the wind tunnel.

All models were sting mounted and the forces and moments were measured by means of electrical strain-gage balances. For the models tested in the 1- by 3-foot and 10- by 14-inch wind tunnels the balances measuring the normal and axial forces were housed in the sting-support structure and pitching moments were indicated by strain gages mounted on the stings. The forces on the sting support were essentially eliminated for these balances by shrouds extending to within 0.040 inch of the base of the model. In the 6- by 6-foot wind tunnel a six-component balance housed inside the model was used.

Models

Sketches of the various models tested are shown in figures 1, 2, and 3. The models tested in the first phase of the investigation are shown in figure 1. These five models consisted of a cylindrical body fitted with either a conical or hemispherical nose and one of three sets of stabilizing surfaces. The over-all fineness ratio of the body for each of the models was 16. Models A, B, and D had stabilizers that simulated folding surfaces which would make it possible to store and launch the missile from a tube. The stabilizing surfaces on model A simulated the fins on a current folding-fin aircraft rocket. The stabilizing surfaces on models B and D simulated 90° segments of the body surface flared 20° into the air stream. The length of these segments was 10 percent of the total body length. The stabilizing surface used on models C and E was the frustum of a cone having the same flare angle and length as the segments of model B. This stabilizing surface was tested in order to indicate the difference in effectiveness of the flared segments and full-cone stabilizing surfaces. It should be noted that for models A, B, and D, the stabilizing surfaces were rotated 45° from the pitch plane. Photographs of models C and D are shown in figure 4.

The control moments on models A, B, and C were developed by deflecting a portion of the body surface near the nose into the air stream. The

control surfaces for models D and E were portions of the surface of the nose that could be deflected into the air stream. Deflection angles of 0°, 10°, 20°, and 30°, measured from the fully retracted position, were tested.

The model for the second phase of the investigation, model F, retained the same basic configuration as model D, as shown in figure 2. However, control was accomplished by deflecting the stabilizing segments from their original flare angle. This model was tested with the pitch plane coinciding with the plane of symmetry of one set of stabilizing surfaces. The two surfaces lying in the pitch plane were deflected equal amounts for control purposes, that is, one surface was deflected outward as much as the opposite surface was retracted. The effect of a variation in segment length and initial flare angle on the stability and control of the configuration was investigated. The values used are tabulated below.

Segment length (percent of body length)	Initial flare angle, deg
10.0	10, 15, 20
18.3	10, 15
26.2	10, 15

Maximum control deflection (measured from the initial flare angle) varied with the stabilizing surfaces and was equal to the initial flare angle. Thus for maximum control deflection the angle of one control, measured from the body surface, was twice the initial flare angle while the opposite control was retracted to the body surface.

A sketch of the model tested in the third phase of the investigation, model G, is shown in figure 3. Since this phase of the investigation was conducted in both the 6- by 6-foot supersonic and 10- by 14-inch hypersonic wind tunnels, two separate models were used. The body diameters of these two models are noted in figure 3. The plane of symmetry of one set of stabilizing surfaces coincided with the pitch plane for this model and control was accomplished in the same manner as for model F. Control deflections of 0°, 6°, 12°, and 17° measured from the initial flare angle were tested.

It should be noted that, with one exception, solid blocks of wood or metal, simulating bellows-deflected controls, were used for the controls involving deflected portions of the body surface. The exception was the nose control used on models D and E. This control was built of a 1/16-inch sheet of Duralumin supported by a 1/4-inch-thick wedge of Duralumin extending 86 percent of the length of the control. The surface of the control was contoured so that when fully retracted it formed a portion of the surface of the conical nose. A rear view of this control is shown in the inset in figure 4(b).

In order to evaluate the performance of the wingless missiles, results are also presented for a conventional winged, cruciform missile. The geometrical characteristics of this missile are given in figure 5.

TESTS AND PROCEDURE

The ranges of the variables for the various models are tabulated below.

Models A through E

M	2.44	3.35
α	-8° to 24°	-8° to 24°
δ	0° to 30°	0° to 30°
R	12.7×10^6	13.4×10^6

(1- by 3-foot supersonic wind tunnel)

Model F

M	3.35
α	-3° to 24°
δ	Varied with control surface
R	13.4×10^6

(1- by 3-foot supersonic wind tunnel)

Model G

	M = 1.76	M = 2.0	M = 2.2	M = 3.0	M = 4.24	M = 5.05
α	-6° to 24°	-6° to 24°	-6° to 24°	-3° to 17°	-3° to 17°	-3° to 17°
δ	0° to 17°	0° to 17°	0° to 17°	0° to 17°	0° to 17°	0° to 17°
R	9×10^6	9×10^6	9×10^6	11.8×10^6	10.4×10^6	5.0×10^6
	(6- by 6-foot wind tunnel)			(10- by 14-inch wind tunnel)		

The pressures acting on the base of the bodies were measured during the tests and were used in correcting the drag data to values that would have been measured had free-stream static pressure been acting on the cross-sectional area of the body. Thus the drag coefficients include the effects of base pressure only on the rear face of the stabilizing surfaces.

As can be seen from the information tabulated above, the Reynolds number for the tests of model G at a Mach number of 5.05 was about half of that for the remainder of the investigation. Previous tests of slender bodies in the 10- by 14-inch wind tunnel (where the present tests were conducted) have indicated that a boundary-layer trip was necessary to prevent laminar separation of the flow over the rear portion of the body in this Mach number and Reynolds number range. For this reason a boundary-layer trip was installed on the nose of the model. The data presented for model G at Mach numbers of 3.0, 4.24, and 5.05 were obtained with the boundary-layer trip in place. For comparison purposes several runs were made at these Mach numbers with the trip removed. The increase in axial-force coefficient due to the presence of the boundary-layer trip averaged about 0.05 and was relatively independent of angle of attack.

The stability and trim characteristics of an aircraft configuration are dependent to a considerable degree on the assumed location of the center of gravity. For an evaluation of several configurations, it is therefore necessary to establish some criterion for the selection of the center-of-gravity locations in order that the results be comparable. Because of the nonlinear nature of the pitching-moment curves, there is a considerable change in the stability of the models through the range of trim lift coefficients. Thus it was not possible to select a center-of-gravity location for a given model which would result in a specified stability for all values of trim lift coefficient. Instead, the criterion used to select the center-of-gravity location required that through the range of trim lift coefficients, the static stability of the models, C_{m_α}, be equal to or greater than a specified minimum value. In order to find the center-of-gravity position that satisfied this requirement, the data were cross-plotted to find the trim lift coefficients at which minimum stability occurred for a series of center-of-gravity positions. The value of C_{m_α} was then determined at each of these points and plotted as a function of center-of-gravity position. From this plot the center of gravity was selected to give a minimum value of C_{m_α} of -0.10. For models A through E two such locations were determined, one for each Mach number tested. The more forward of the two positions was selected as the center-of-gravity position to be used in the moment calculations.

The above procedure was also followed in selecting the center-of-gravity locations for each of the models tested under the designation model F. However, the interpolation necessary to find the trim lift coefficients for minimum stability for these models was not as accurate as that for models A through E, since only two control deflections were investigated for model F. The manner in which these inaccuracies in the interpolation affect the data are mentioned in the following section. The choice of the center-of-gravity location for model G is also discussed in the following section.

The center of gravity for the winged missile used for comparison purposes was selected such that this missile also had a minimum value of C_{m_α} of -0.10; it was located 53.5 percent of the body length from the nose.

PRECISION OF DATA

In a static force test such as the present investigation, the values often used for the accuracy of the data are those obtained from the least readings of the instruments used in the investigation. Since the scatter in repeated measurements exceeds these values, it was felt that this information is not worth presenting. Instead, any repeat points that were obtained have been included in the tabulated results. The reader can estimate the accuracy of the data from the scatter in these values.

RESULTS AND DISCUSSION

In the following discussion only a portion of the test results will be considered in detail. These data are presented in figures 6 through 18. The results of the entire investigation are tabulated in tables I through IX.

Missiles Having Nose Controls

The results of the first phase of the investigation are shown in figures 6 through 10. Angle of attack, drag, and pitching-moment coefficients are plotted versus lift coefficient for models A through E. The nonlinear character of the lift and pitching-moment curves for all models is immediately apparent. This phenomenon in the lift curves is primarily due to viscous crossflow forces. The pitching-moment curves, however, show a higher degree of nonlinearity than is present in the lift curves. This is due primarily to the relatively large movement of the center of pressure with angle of attack that is characteristic of slender bodies. By subtracting the tabulated values of tail-off pitching moments from the tail-on values, it can be shown that the moment contributions of the stabilizing surfaces of models B and C are slightly nonlinear. However, the nonlinearities arising from this source are small compared to those caused by the center-of-pressure movement on the body alone.

The effectiveness of the three sets of stabilizing surfaces can be seen in figures 6 through 8. A measure of the effectiveness of the stabilizing surfaces is the location of the center of gravity necessary to give the model adequate stability under the conditions specified in a previous section. Under these conditions the more effective the stabilizing surfaces, the farther aft will be the center of gravity. Tabulating the center-of-gravity locations we have:

Model	Center-of-gravity location
A	0.492l
B	.410l
C	.502l

It can be seen that the stabilizer effectiveness was greatest for the conical flare of model C and least for the segmented flare of model B.

A measure of the effectiveness of the two control surfaces tested is shown in figure 11. Here the pitching-moment coefficient at $\alpha = 0^\circ$ has been plotted as a function of control deflection. In order to eliminate the effect of moment center location on the pitching-moment contributions of the two controls, the moment center for these data was arbitrarily set at 50.0 percent of the body length from the nose. The data presented in this figure were taken from tests of the hemispherical- and conical-nosed models with conical-flare stabilizing surfaces. Ideally, control effectiveness should be obtained from tail-off data, since the presence of various stabilizing surfaces in the flow behind the control will affect the results in varying degrees. However, only the hemispherical-nosed model was tested with the tail-off; hence, tail-off comparisons cannot be made. In order to give some idea of the effect of the conical stabilizer on the control effectiveness, the data for the hemispherical-nosed model, tail-off, are shown in the figure. Also presented are the theoretical values for the pitching-moment coefficient calculated using Newtonian impact theory (ref. 5).

The theoretical results show that, despite its smaller surface area and moment arm, the control on the conical-nosed body is more effective than that on the hemispherical-nosed body for deflections up to about 20°. The theory predicts that the force on both controls varies as the sine squared of the angle to the air stream. As a result, the initial angle of the conical nose control leads to a higher effectiveness for this control than for the hemispherical nose control at the lower deflections. As deflection increases, however, the advantage of the conical nose control is overcome by a greater reduction in the moment arm of the force for this control than that for the hemispherical nose control. Thus the theory indicates a higher effectiveness for the hemispherical nose control at the higher deflections.

The experimental results show fair agreement with theory for the nose control. The results for the hemispherical nose control are, in general, appreciably below the theoretical values. This discrepancy is due primarily to the effect of pressure losses through the strong shock wave ahead of the hemispherical nose. Comparison of the tail-on and tail-off results for the hemispherical nose control indicates that the conical flare stabilizer has little effect on the control moments.

[redacted]

One of the most important quantities in the evaluation of the performance of a missile is the maximum trimmed lift that can be developed. A plot of this quantity as a function of Mach number is shown in figure 12 for the five configurations tested here. Values for a variable-incidence, cruciform-winged missile are also shown for comparison purposes. The data for this missile were obtained from wind-tunnel and flight-test results given in references 6 and 7. The results for the winged missile represent the normal and lateral trimmed lift coefficients determined by control deflections of 17° and 13°, respectively. The control deflections were limited to these values by mechanical interference between wing panels. The maximum control deflection for the wingless missile was arbitrarily set at 30° from the fully retracted position.

It can be seen that the trimmed lifts for the wingless missiles are appreciably lower than those for the winged missile, although the trend of the latter is toward lower values at the higher Mach numbers. The pronounced change in trimmed lift capability with Mach number for models A and C can be attributed in large part to the change in effectiveness of the stabilizing surfaces with Mach number. By subtracting the tail-off data from the tail-on results, it can be shown that the moment contribution of the simulated folding fins of model A decreases markedly with an increase in Mach number, whereas that for the conical flare of model C increases somewhat. The moment contribution of the flared segments of model B remained essentially constant for the two Mach numbers tested. These changes in stability are, of course, reflected in the maximum trimmed lift attained by the models. It should be noted that the hemispherical-nosed body with tail off showed an increase in stability with increasing Mach number which added to the effect of the increased stability of the conical flare on the trimmed lift coefficient for model C. Since tail-off data were not obtained for the conical-nosed models, the effects of Mach number on the separate contributions of the body and stabilizing surfaces are not known. However, it can be seen that Mach number had a smaller effect on trimmed lift for these models than for those with the hemispherical nose.

The question arises as to the importance of the reduced trimmed lift capabilities and the nonlinearities in lift and pitching moment on the performance of the missile. The significance of these factors on the tracking performance of the missile was investigated in a simulation study of a tracking problem utilizing the missile as a beam rider. Model D was used for the study with a slightly different center-of-gravity position. The results of this investigation are presented in reference 8. To summarize briefly here: The problem studied was that of tracking a maneuvering target with radar glint noise present. Time histories of the motion of the missile were obtained along with a root mean square value of the radial miss distance. In order to establish a frame of reference with which to evaluate the performance of the wingless configuration, results were also presented for a conventional winged, cruciform missile. The

results of the simulation study showed that the tracking capabilities of the wingless missile at Mach numbers of 2.44 and 3.35 compared favorably with those of the cruciform missile at a Mach number of 1.5.

In figure 13, the drag at zero lift and at maximum trimmed lift is plotted as a function of Mach number for the missiles tested in the first phase of the investigation. It should be noted again that the drag values are those that would have been measured if free-stream static pressure had been acting on the body cross-sectional area at the base. Since the pressures in the region of the base during flight, both powered and gliding, may be considerably different than free-stream static pressure, the drag coefficients presented here could be considerably different than flight values. However, the comparisons that follow are felt to be valid since the same method of correcting the base drag was used for all models. The relatively high drag of the wingless missiles at zero lift shown in figure 13(a) is due to the blunt nose shape and/or blunt stabilizing surfaces used. In the trimmed condition (fig. 13(b)), the drag of the wingless missiles is comparable to that of the winged missile. For both types of missiles a sizable portion of the drag in the trimmed condition is due to the deflection of the control surfaces. One method of reducing the control drag for the wingless missiles would be to eliminate the nose control and use the flared segments of models B and D for both stabilization and control in a manner similar to that suggested by Eggers and Syvertson in reference 4. In this arrangement the flared segments would be deflected from their initial flare angle to produce the control moments on the airframe. The advantage of such an arrangement lies in the fact that the deflected tail control is at a lower angle to the air stream in the trimmed condition than is the deflected nose control. Thus the drag in the trimmed condition would be appreciably lower for the missile with the tail control than for the missile with the nose control at the same trim lift.

Missiles Having Tail Controls

As a result of the above considerations, a study of the aerodynamic characteristics of the tail control arrangement was undertaken. The second phase of the investigation covered tests of a model using tail control; the effects of the geometry of the control on the maximum trimmed lift, drag, and stability of the model were studied. The model (model F), as previously described, was similar to model D with the exception that the flared segments were used both for stability and control and the segment length and initial flare angle were varied during the investigation. The tests were made only for the zero and maximum-control-deflection conditions since it was felt that intermediate control deflection data were not essential in the initial evaluation. It may be worth while to mention here again that the upper and lower controls were moved equal amounts to produce a control moment, the upper being extended while the

[redacted]

lower was retracted. Thus the maximum deflection for each set of flared segments tested was limited to the angle at which the lower control was flush with the body surface, that is, the initial flare angle. The investigation was made at $M = 3.35$ only. The data from these tests were tabulated in table VII.

In order to allow rapid evaluation of the effects of segment length and initial flare angle on the aerodynamic characteristics of the missile, a summary plot of several aerodynamic parameters is given in figure 14. Figure 14(a) shows the effect of variation in c and δ_f on the maximum trimmed lift coefficient and the corresponding drag coefficient while figure 14(b) shows the effect of these quantities on the center-of-gravity location for a given minimum stability as specified in the previous section. It should be noted that in order to draw the curves of figure 14 from the wind-tunnel data, it was first necessary to plot the parameter involved as a function of c with δ_f constant. From these curves, the values of c and δ_f were picked off and plotted in figure 14. Since a limited number of combinations of c and δ_f were tested, a considerable amount of interpolation was necessary to draw the curves of figure 14 with a resulting compromise in the accuracy of the results. It is felt, however, that these curves are still useful in indicating the effect of the geometry of the configuration on the aerodynamic characteristics of the model.

Examination of figure 14(a) shows that the lines of constant trim lift and trim drag are nearly parallel over a considerable range of values of c and δ_f. In other words the trim lift-drag ratio is nearly constant for this range of c and δ_f. It can also be seen that the trim lift-drag ratio is nearly constant regardless of the trim lift. Thus, various combinations of c and δ_f will give a specified maximum trim lift coefficient and for these the trim lift-drag ratio will be approximately the same.

In order to determine the Mach number range over which the curves of figure 14 might be valid, a configuration was selected for tests at Mach numbers from 1.76 to 5.05. Since it was found that there is a fairly wide range of values of c and δ_f for which the trim lift-drag ratio is nearly constant, the choice of the configuration for tests in this Mach number range was somewhat arbitrary. A segment length of 13.1 percent of the body length and an initial flare angle of 17° was selected and this model was designated model G. The center-of-gravity location for the model was determined from figure 14(b) and was placed 58.5 percent of the body length from the nose. The third phase of the investigation covered tests of this model over a Mach number range from 1.76 to 5.05.

The longitudinal characteristics of model G are shown in figure 15. It is immediately apparent that the center of gravity specified by figure 14(b) does not give the required minimum stability. One possible explanation of this discrepancy was pointed out in the previous section

where the inaccuracies in determining the trim point for minimum stability of model F were mentioned. Since data were obtained for only the zero and maximum control deflections, linear interpolation was used to determine the trim point for minimum stability. When this procedure was followed for model G, the data obtained at the intermediate control deflections showed that the linear interpolation carried out for the data of model F was not a good approximation. Thus it is not surprising that figure 14(b) does not accurately predict the center-of-gravity location for the specified minimum stability. However, it is felt that figure 14(b) is useful in indicating the effect of the geometry of the flared segments on the relative stability of this configuration. If the center of gravity is moved forward to a point 49.0 percent of the body length from the nose, the minimum value of C_{m_α} at M = 3.00 will be -0.10. With this center-of-gravity location the double trim points seen in figure 15 at the lower Mach numbers disappear and the nonlinearities in the pitching-moment curves are reduced somewhat due to the increased stability.

In figures 16 and 17 the trim lift capabilities and drag characteristics, respectively, are plotted as a function of Mach number for the center of gravity located 58.5 percent of the body length from the nose. Reference to figure 14(a) shows that, for the proper combination of c and δ_f, the values of trim lift and drag predicted by that figure agree fairly well with those measured on model G for Mach numbers from about 3 to 5. However, below a Mach number of 3.0 both the trim lift and trim drag increase considerably primarily because of the decrease in stability of the model. With the center of gravity in this position the trim lift and drag are comparable to those of the winged missile.

Also shown in the two figures are the maximum trimmed lift and drag for the wingless missile when the center of gravity is moved forward to 0.490ℓ to achieve the specified stability. It is seen that this movement in center-of-gravity location reduces both the maximum trimmed lift and drag by a factor of approximately 2 for Mach numbers from 3.00 to 5.05 and by an even greater amount in the lower Mach number range. Upon comparison of the results at this center-of-gravity location with those of model D, it can be seen that although the trim lift for the tail control model is somewhat lower than that for the nose control model, the trim drag is appreciably lower. Thus, control drag has been reduced by use of the tail control with some sacrifice in maximum trimmed lift capability.

In addition to the usual longitudinal data, some information was obtained with model G at various roll angles. These data are tabulated in table IX.

Earlier in this section a comparison between Newtonian impact theory and experiment was made for the nose control. It is also of interest to make this comparison for the tail control. With this in mind, a portion of the lateral data obtained on model G is presented in figure 18. The lateral coefficients C_Y, C_n, and C_ℓ were selected for this comparison

with theory since the body makes no direct contribution to these coefficients at zero sideslip. Thus these data show the effect of the control surfaces alone and the theoretical results can be compared directly with the experimental values.

Shown in figure 18 are plots of the lateral coefficients as a function of angle of attack for the model with maximum control deflection at several roll angles. Also shown in the figure are theoretical values for the coefficients based on impact theory. Agreement between theory and experimental values of side-force coefficient is very good near $\alpha = 0^\circ$. The side-force coefficient also shows fair agreement for $\varphi = 90^\circ$ up to $\alpha = 21^\circ$ where there is a relatively abrupt change in slope for the experimental values. The reason for the change in slope is not fully understood at the present time but could be due to the effect of the vortices shed from the nose at high angles of attack on the flow around the control surfaces. At $\varphi = 45^\circ$, the magnitude of C_Y decreases much more rapidly with increasing angle of attack than is indicated by the theory. A possible explanation for this discrepancy will be mentioned shortly.

The values of yawing-moment coefficient plotted in figure 18 show that the theory slightly underestimates the magnitude of C_n near $\alpha = 0^\circ$. As would be expected, the variation of C_n with angle of attack is approximately that shown by C_Y and the deviation from the theoretical curve is comparable to that mentioned above. The values of rolling-moment coefficient predicted by the theory are considerably below the experimental results. This discrepancy is probably due, in large part, to the assumption in the theory that the pressure coefficient on lee surfaces is zero. The rolling moments are, of course, developed by loads on the flat side surfaces of the controls. The pressure coefficient on the lee sides of these surfaces is probably something less than zero giving rise to larger rolling moments than predicted by the theory. This could also account for the lack of agreement between theory and experiment for the side-force coefficients at $\varphi = 45^\circ$. A pressure coefficient less than zero on the lee surface of the deflected control would result in a lower side-force coefficient than that predicted by Newtonian theory. Such an explanation is at least consistent with the results in figure 18.

It is apparent that the agreement between theory and experiment is better for the tail control than for the nose controls. One reason for this has been pointed out previously, that is, the effect of nose shape on the dynamic pressure in the region of the nose controls. Another factor which could contribute to the differences between theory and experiment for the two types of controls is the fact that the flow behind the nose control can have some influence on the forces and moments through loads developed on the body. This is not true, however, of the tail control.

CONCLUSIONS

An experimental investigation of several wingless missile configurations has been made. In order to establish a frame of reference with which to evaluate the performance of these configurations, results are also presented for a conventional winged, cruciform missile. The following conclusions can be drawn from the results of the investigation:

1. With the center-of-gravity location chosen such that the minimum value of the pitching-moment-curve slope at trim was -0.10, the maximum trimmed lift coefficients for the wingless configurations were, in general, somewhat lower than those for the winged missile.

2. The drag of models using the nose control was somewhat higher than that for the winged missile for both the zero and maximum trimmed lift conditions.

3. The use of flared segments of the body surface as both stabilizing and control surfaces improves the trim lift-drag ratio over the models using nose control, with some sacrifice in maximum trimmed lift capability.

4. Newtonian impact theory predicts the side-force and yawing-moment coefficients due to lateral deflection of the tail control with reasonable accuracy at angles of attack near zero. The rolling-moment coefficients and side-force and yawing-moment coefficients at the higher angles of attack are not in good agreement with the theory. The theoretical values of pitching-moment coefficient due to deflection of the control on the conical nose were in fair agreement with the experimental results, whereas this comparison for the control behind the hemispherical nose was poor.

Ames Aeronautical Laboratory
National Advisory Committee for Aeronautics
Moffett Field, Calif., Oct. 22, 1957

REFERENCES

1. Katzen, Elliott D., and Jorgensen, Leland H.: Aerodynamics of Missiles Employing Wings of Very Low Aspect Ratio. NACA RM A55L13b, 1956.

2. Jorgensen, Leland H., and Katzen, Elliott D.: Wing-Body Combinations With Wings of Very Low Aspect Ratio at Supersonic Speeds. NACA RM A56G16, 1956.

3. Lazzeroni, Frank A.: Investigation of a Missile Airframe With Control Surfaces Consisting of Projecting Quadrants of the Nose Cone. NACA RM A53L21, 1954.

4. Eggers, A. J., Jr., and Syvertson, Clarence A.: Experimental Investigation of a Body Flare for Obtaining Pitch Stability and a Body Flap for Obtaining Pitch Control in Hypersonic Flight. NACA RM A54J13, 1955.

5. Grimminger, G., Williams, E. P., and Young, G. B. W.: Lift on Inclined Bodies of Revolution in Hypersonic Flow. Jour. Aero. Sci., vol. 17, no. 11, Nov. 1950, pp. 675-690.

6. Anon.: Normal Force and Pitching Stability and Control Characteristics for Sparrow 15-C and 15-D Configurations. Rep. MTM-343, Douglas Aircraft Co., Aug. 9, 1951.

7. Delameter, H. D., Buell, D. R., and Mixon, M. S.: Summary of XAAM-N-2 Sparrow Missile; Performance and Stability and Control Characteristics. Rep. No. SM-13907, Douglas Aircraft Co., Oct. 29, 1951.

8. Lessing, Henry C., and Reese, David E., Jr.: A Simulation Study of a Wingless Missile. NACA RM A55L06, 1956.

TABLE I.- EXPERIMENTAL RESULTS FOR MODEL A; C.G. AT 0.492$\bar{c}$

δ_e, deg	α, deg	C_L	C_D	C_m	δ_e, deg	α, deg	C_L	C_D	C_m
(a) M = 2.44									
0	-8.5	-1.60	1.45	5.60	20	-8.6	-1.66	1.59	5.95
	-6.3	-1.09	1.32	4.28		-6.3	-1.11	1.46	4.71
	-3.0	-.46	1.20	1.97		-2.9	-.37	1.35	2.71
	.2	.03	1.18	-.12		.4	.23	1.37	1.96
	.2	.03	1.16	-.10		.4	.22	1.36	.97
	3.6	.48	1.18	-1.96		.4	.21	1.37	-----
	6.9	1.13	1.32	-4.37		3.8	.79	1.45	-.71
	10.2	1.91	1.51	-5.95		7.2	1.47	1.62	-2.78
	13.5	2.97	1.91	-7.14		10.5	2.30	1.92	-4.41
	16.8	4.16	2.64	-8.72		13.9	3.40	2.44	-5.63
	20.1	5.62	3.51	-11.51		17.3	4.70	3.24	-7.02
	23.4	7.29	4.79	-16.06		20.7	5.98	4.24	-9.64
						24.1	7.32	5.51	-12.75
10	-8.3	-1.68	1.49	5.74					
	-6.1	-1.14	1.38	4.52	30	-8.3	-1.65	1.83	6.87
	-2.9	-.44	1.26	2.30		-6.0	-1.05	1.71	5.64
	.3	.10	1.23	.23		-2.6	-.23	1.68	3.69
	.3	.07	1.21	.38		.7	.45	1.72	2.09
	.3	.06	1.23	.46		.7	.46	1.73	2.09
	3.6	.57	1.28	-1.56		.7	.45	1.45	2.18
	6.9	1.22	1.40	-3.83		4.1	1.12	1.90	.38
	10.2	2.04	1.64	-5.63		7.5	1.88	2.08	-1.36
	13.4	3.20	2.11	-6.85		10.9	2.73	2.51	-2.92
	16.7	4.46	2.80	-8.40		14.3	4.02	3.20	-4.13
	20.0	5.85	3.76	-11.00		17.7	5.25	4.11	-5.97
	23.3	7.28	4.98	-14.97		21.2	6.56	5.23	-8.89
						24.5	7.89	6.63	-12.38
(b) M = 3.35									
0	-8.3	-1.59	1.52	3.60	10	16.3	3.97	2.62	-6.91
	-6.1	-.99	1.36	2.58		19.6	5.21	3.47	-9.58
	-2.9	-.43	1.22	1.09		22.8	6.60	4.58	-13.21
	.3	-.04	1.21	-.26					
	.3	-.03	1.18	-.23	20	-7.8	-1.48	1.57	4.00
	.3	.04	1.18	-.11		-5.7	-.94	1.43	2.97
	3.5	.33	1.23	-1.49		-2.4	-.32	1.32	1.78
	3.5	.33	1.21	-1.47		.7	.17	1.34	.71
	6.7	.85	1.31	-2.96		.7	.16	1.33	.73
	9.9	1.69	1.56	-4.46		3.9	.77	1.44	-.70
	9.9	1.68	1.54	-4.34		7.2	1.23	1.64	-1.20
	13.2	2.73	1.91	-5.93		10.4	2.05	1.93	-2.02
	13.2	2.73	1.89	-5.98		13.6	3.05	2.35	-2.74
	16.4	3.93	2.47	-8.16		16.8	4.17	3.02	-4.41
	16.4	3.92	2.47	-8.24		20.1	5.37	3.90	-7.24
	19.6	5.24	3.31	-10.85		23.3	6.69	5.08	-10.77
	19.6	5.22	3.29	-10.80					
	22.8	6.63	4.39	-14.00	30	-8.1	-1.38	1.66	4.81
						-5.9	-.80	1.55	3.75
10	-8.4	-1.54	1.52	3.71		-2.6	-.14	1.47	2.59
	-6.2	-1.00	1.38	2.65		.6	.41	1.56	1.69
	-3.0	-.39	1.27	1.32		.6	.44	1.55	1.47
	.1	.04	1.23	-.02		.6	.17	1.48	-----
	.1	.04	1.22	.03		3.9	.98	1.73	.91
	.1	.02	1.22	.16		7.2	1.57	2.01	.48
	3.4	.45	1.29	-1.14		10.5	2.37	2.36	.23
	6.6	.98	1.44	-2.56		13.8	3.34	2.88	-.24
	6.6	.98	1.41	-2.45		17.1	4.39	3.60	-2.10
	9.8	1.80	1.65	-3.79		20.4	5.45	4.51	-4.89
	13.1	2.84	2.04	-5.10		23.7	6.61	5.65	-8.77

TABLE II.- EXPERIMENTAL RESULTS FOR MODEL B; C.G. AT 0.410$\bar{c}$

δ_e, deg	α, deg	C_L	C_D	C_m	δ_e, deg	α, deg	C_L	C_D	C_m
(a) M = 2.44									
0	-8.7	-1.07	1.64	3.12	20	-8.5	-1.07	1.74	3.17
	-6.5	-.73	1.56	2.63		-6.3	-.69	1.68	2.68
	-3.1	-.39	1.45	1.97		-2.9	-.23	1.61	2.10
	.1	.00	1.45	.07		.4	.19	1.62	.86
	.1	.01	1.37	.06		.4	.17	1.60	.98
	.1	-.01	1.40	.26		.4	.14	1.59	1.12
	3.4	.32	1.43	-1.33		3.7	.50	1.68	.55
	6.8	.66	1.54	-2.10		7.1	.96	1.81	-.65
	10.1	1.24	1.66	-2.96		10.5	1.57	2.01	-1.60
	13.4	2.18	1.84	-4.09		13.8	2.58	2.40	-2.84
	16.8	3.30	2.47	-6.69		17.2	3.63	3.03	-5.14
	20.1	4.59	3.36	-11.09		20.6	4.89	4.00	-9.41
	23.4	5.64	4.34	-----					
10	-8.6	-1.10	1.63	3.10	30	-8.2	-.98	1.85	3.59
	-6.3	-.71	1.64	2.54		-8.2	-.96	1.94	3.60
	-3.0	-.32	1.53	1.86		-6.0	-.59	1.82	3.30
	.3	.04	1.48	.48		-2.7	-.11	1.79	2.78
	.3	.05	1.46	.39		.6	.37	1.84	1.63
	.3	.04	1.46	.42		.6	.38	1.84	1.55
	3.6	.37	1.46	-.68		.6	.37	1.80	1.71
	7.0	.79	1.58	-1.86		3.9	.73	1.97	1.51
	10.4	1.36	1.74	-2.64		7.2	1.16	2.14	.70
	13.7	2.28	2.06	-3.76		13.9	2.78	2.81	-1.66
	17.1	3.39	2.59	-6.23		17.2	3.81	3.50	-3.95
	20.4	4.61	3.47	-10.28		20.6	4.92	4.33	-7.88
	23.8	5.43	4.45	-----					
(b) M = 3.35									
0	-8.1	-1.12	1.50	3.15	20	-8.0	-1.10	1.57	3.88
	-5.9	-.73	1.43	2.45		-5.8	-.68	1.51	2.77
	-2.7	-.37	2.59	1.53		-2.6	-.28	1.43	2.09
	.3	-.02	1.25	-.07		.4	.12	1.45	.65
	.3	-.04	1.19	.03		.4	.12	1.35	.69
	.3	-.02	1.20	-.21		.4	.13	1.32	.62
	.3	-.04	1.26	.04		3.6	.50	1.49	-.52
	3.3	.33	1.28	-1.99		6.8	.93	1.67	-1.49
	6.5	.66	1.45	-2.99		10.1	1.48	1.87	-1.77
	9.4	1.24	1.60	-3.94		13.5	2.36	2.37	-3.71
	13.1	2.07	1.94	-5.98		16.9	3.31	2.90	-6.60
	16.4	3.05	2.46	-9.18		20.3	4.27	3.67	-10.08
	19.4	4.10	3.15	-12.85		23.6	5.28	4.65	-14.60
	23.3	5.23	4.13	-16.74					
10	-7.7	-1.14	1.50	3.52	30	-7.3	-1.02	1.67	4.32
	-5.9	-.74	1.46	2.59		-5.5	-.57	1.65	3.29
	-2.7	-.34	1.35	1.71		-2.5	-.13	1.61	2.63
	.3	.02	1.31	.09		.6	.29	1.64	1.46
	.3	.01	1.24	.15		.6	.29	1.52	1.35
	.3	.00	1.26	.14		.6	.31	1.47	1.25
	.3	.02	1.21	.12		3.8	.75	1.79	.29
	3.4	.35	1.33	-1.29		7.1	1.21	1.99	-.37
	6.6	.76	1.51	-2.70		10.5	1.76	2.22	-.16
	9.8	1.36	1.63	-3.66		13.9	2.62	2.68	-2.24
	9.8	1.36	1.63	-3.66		17.2	3.48	3.34	-5.04
	13.2	2.18	2.13	-5.68		20.6	4.35	4.12	-8.68
	16.6	3.13	2.57	-8.42		23.9	5.31	5.12	-13.34
	20.0	4.12	3.27	-11.87					
	23.3	5.18	4.22	-16.29					

[redacted]

TABLE III.- EXPERIMENTAL RESULTS FOR MODEL C; C.G. AT 0.502$\bar{c}$

δ, deg	α, deg	C_L	C_D	C_m	δ, deg	α, deg	C_L	C_D	C_m
(a) M = 2.44									
0	-8.1	-1.13	2.33	2.67	20	-8.1	-1.17	2.28	2.99
	-5.9	-.81	2.24	2.68		-5.8	-.77	2.33	2.77
	-2.6	-.51	2.09	2.68		-2.5	-.33	2.23	2.76
	.3	.00	2.10	.05		.5	.14	2.27	1.23
	.3	.02	2.09	-.10		.5	.19	2.27	1.04
	3.4	.44	2.19	-2.12		.5	.17	2.25	1.14
	6.6	.73	2.29	-2.17		3.7	.57	2.33	.22
	9.9	1.33	2.37	-2.59		6.9	1.02	2.50	-.47
	13.4	2.32	2.61	-3.35		10.3	1.67	2.65	-.86
	17.0	3.45	3.14	-4.69		13.9	2.68	3.08	-1.53
	20.5	5.06	3.54	-8.60		17.4	3.73	3.64	-2.82
						21.0	5.01	4.61	-5.97
						24.6	6.14	5.93	-8.71
10	-8.1	-1.15	2.32	2.71					
	-5.9	-.80	2.26	2.63	30	-8.0	-1.05	2.50	3.33
	-2.6	-.44	2.12	2.65		-5.7	-.66	2.42	3.45
	.4	.01	2.13	.64		-3.1	-.16	2.42	3.47
	.4	.03	2.18	.61		.7	.35	2.47	2.11
	.4	.07	2.16	.53		.7	.36	2.48	2.06
	3.5	.44	2.19	-1.10		.7	.38	2.42	2.01
	6.7	.81	2.32	-1.62		3.3	.80	2.58	1.71
	10.0	1.41	2.45	-2.12		6.6	1.22	2.79	1.43
	13.6	2.44	2.75	-2.48		10.0	1.85	3.02	1.25
	17.2	3.56	3.33	-4.19		13.6	2.89	3.47	.58
	20.7	4.93	4.01	-7.33		17.1	3.07	3.87	----
	24.6	6.02	5.49	-9.76					
(b) M = 3.35									
0	-8.0	-1.31	1.99	3.58	20	-7.9	-1.27	2.04	4.14
	-5.8	-.86	1.96	2.84		-5.8	-.84	2.02	3.37
	-2.7	-.50	1.86	2.27		-2.6	-.40	1.96	2.80
	.3	-.04	1.86	-.05		.4	.10	2.07	.97
	.3	-.05	1.68	0		.4	.09	1.77	1.01
	.3	-.06	1.76	.04		.4	.10	1.75	.92
	3.3	.45	1.78	-2.76		3.5	.58	1.94	-.62
	6.4	.82	1.98	-3.70		6.7	1.06	2.15	-1.73
	9.6	1.40	2.28	-4.52		10.0	1.71	2.40	-2.07
	13.0	2.34	2.54	-6.30		13.4	2.63	2.84	-3.47
	16.3	3.43	3.06	-9.15		16.7	3.66	3.57	-6.05
	19.6	4.64	3.60	-12.43		20.0	4.66	4.44	-9.19
	23.0	5.76	4.86	-15.58		23.4	5.90	5.14	-12.81
10	-8.0	-1.27	1.99	3.64	30	-7.8	-1.19	2.17	4.77
	-5.8	-.86	1.95	2.92		-5.7	-.73	2.13	4.01
	-2.6	-.45	1.86	2.28		-2.4	-.25	2.06	3.40
	.3	-.00	1.86	.31		.6	.29	2.07	1.74
	.3	-.00	1.68	.31		.6	.30	2.07	1.78
	.3	-.00	1.75	.30		.6	.28	2.24	1.89
	3.4	.46	1.80	-1.93		3.8	.83	2.22	.37
	6.5	.90	2.03	-3.25		7.0	1.32	2.47	-.01
	9.8	1.50	2.33	-3.90		10.4	1.93	2.27	.43
	13.1	2.45	2.80	-5.60		13.7	2.86	3.16	-1.29
	16.4	3.48	3.17	-8.09		17.0	3.82	4.00	-3.68
	19.7	4.55	3.98	-11.26		20.3	4.54	4.76	-7.10
	23.1	5.73	5.01	-14.88		23.6	5.80	5.97	-11.26

TABLE IV.- EXPERIMENTAL RESULTS FOR MODEL D; C.G. AT 0.506$\bar{c}$

δ, deg	α, deg	C_L	C_D	C_m	δ, deg	α, deg	C_L	C_D	C_m
(a) M = 2.44									
0	-8.0	-1.15	.85	2.01	20	-8.1	-.98	1.17	3.05
	-5.9	-.80	.79	1.59		-5.6	-.59	1.17	2.82
	-2.7	-.38	.70	1.03		-2.4	-.08	.98	2.33
	.3	-.01	.69	-.03		.7	.32	1.02	1.82
	.3	-.03	.70	.17		.7	.34	1.00	1.77
	.3	.00	.66	.07		3.8	.66	1.06	1.69
	3.4	.37	.68	-.83		3.9	.66	1.06	1.70
	6.6	.81	.78	-1.47		7.1	.97	1.16	2.03
	9.8	1.44	.93	-2.09		7.1	.95	1.17	2.06
	13.3	2.28	1.22	-2.13		10.3	1.64	1.38	.67
	16.7	3.33	1.73	-3.41		13.6	2.39	1.75	.05
	20.1	4.46	2.47	-5.82		17.0	3.35	2.27	-1.57
	23.6	5.67	3.52	-8.41		20.4	4.33	3.01	-3.92
						23.7	5.41	4.01	-6.47
10	-8.0	-1.13	.93	2.43					
	-5.8	-.76	.85	2.14	30	-7.7	-.80	1.28	3.82
	-2.6	-.30	.77	1.48		-5.5	-.35	1.25	3.56
	.4	.10	.82	.68		-2.2	.13	1.26	3.27
	.4	.10	.76	.73		.9	.53	1.33	3.00
	.4	.09	.79	.77		.9	.53	1.31	3.00
	3.6	.43	.83	.29		.9	.53	1.33	2.99
	6.7	.85	.91	-.34		4.1	.84	1.40	3.24
	10.0	1.31	1.09	-.90		7.4	1.13	1.53	3.75
	13.4	2.32	1.42	-1.33		7.4	1.13	1.55	3.83
	16.8	3.35	1.94	-2.75		10.6	1.66	1.73	2.96
	20.2	4.43	2.69	-4.78		13.8	2.50	2.15	1.07
	23.6	5.59	3.68	-8.30		17.2	3.26	2.66	-.43
						20.4	4.18	3.38	-3.20
						23.8	5.03	4.27	-5.79
(b) M = 3.35									
0	-8.0	-1.36	.81	1.82	20	-7.9	-1.12	.93	2.70
	-5.9	-.87	.73	1.25		-5.7	-.64	.87	2.19
	-2.7	-.38	.69	.30		-2.5	-.10	.96	1.87
	.3	-.01	.74	-.24		.6	.30	.87	1.53
	.3	-.01	.57	-.24		.6	.30	.85	1.51
	.3	-.01	.63	-.17		.6	.31	.33	1.53
	.3	.00	.69	-.21		.6	.30	.93	1.60
	3.4	.31	.64	-.87		3.7	.64	.95	1.54
	6.5	.77	.71	-1.50		6.9	.95	1.00	2.02
	9.7	1.45	.89	-2.16		10.1	1.57	1.22	1.03
	13.0	2.32	1.22	-3.29		13.3	2.36	1.69	-.62
	16.3	3.28	1.72	-5.16		16.6	3.20	2.23	-2.62
	19.6	4.26	2.41	-7.38		19.8	4.04	2.90	-5.12
	22.9	5.26	3.29	-9.87		23.0	4.96	3.77	-8.43
10	-8.0	-1.28	.83	2.16	30	-7.7	-.89	1.08	3.45
	-5.8	-.79	.74	1.51		-5.5	-.42	1.07	3.43
	-2.7	-.30	.65	1.06		-2.3	.09	1.13	3.22
	.4	.11	.68	.24		.8	.47	1.28	3.20
	.4	.10	.76	.38		.8	.49	1.19	3.09
	.4	.11	.71	.34		4.0	.77	1.26	3.43
	.4	.11	.72	.28		7.2	1.11	1.34	3.66
	3.5	.41	.73	.30		10.4	1.60	1.55	3.57
	6.7	.86	.79	-.18		13.6	2.31	1.95	1.95
	9.9	1.51	1.00	-.88		16.8	3.08	2.54	-.38
	13.2	2.37	1.43	-2.30		19.9	3.85	3.28	-3.30
	16.4	3.24	1.93	-4.03		23.1	4.71	4.18	-7.40
	19.7	4.15	2.58	-6.33					
	22.9	5.15	3.48	-9.47					

TABLE V.- EXPERIMENTAL RESULTS FOR MODEL E; C.G. AT 0.587$\bar{c}$

δ_f, deg	α, deg	C_L	C_D	C_m	δ_f, deg	α, deg	C_L	C_D	C_m
(a) M = 2.44									
0	-8.0	-1.22	1.45	1.72	20	-7.5	-1.10	1.65	3.04
	-5.8	-.84	1.39	1.56		-5.5	-.66	1.58	2.96
	-2.7	-.43	1.31	1.25		-2.4	-.13	1.60	2.77
	.3	-.03	1.37	.29		.7	.30	1.70	2.31
	.3	.02	1.36	.27		.7	.28	1.63	2.38
	3.4	.41	1.34	-.97		3.8	.59	1.70	2.53
	6.5	.79	1.42	-1.13		7.1	.92	1.76	3.14
	9.8	1.46	1.56	-1.38		10.2	1.65	1.97	1.80
	13.2	2.31	1.84	-1.06		13.5	2.48	2.35	1.22
	16.6	3.44	2.36	-1.76		16.9	3.49	2.89	.10
	19.9	4.60	3.11	-3.33		23.5	5.55	4.64	-3.54
	23.4	5.82	4.19	-4.96					
10	-7.9	-1.26	1.56	2.89	30	-7.6	-.86	1.87	3.91
	-5.7	-.83	1.48	2.66		-5.4	-.43	1.85	3.93
	-2.6	-.38	1.46	1.87		-2.2	-.05	1.90	3.90
	.4	.04	1.52	1.12		.9	.49	2.00	3.76
	.5	.01	1.47	1.29		.9	.48	1.95	3.78
	3.6	.40	1.49	.69		4.1	.76	2.01	4.44
	6.7	.86	1.58	.17		7.3	1.06	2.10	4.99
	10.0	1.56	1.73	-.27		10.5	1.67	2.33	4.10
	13.3	2.42	2.05	-.26		13.7	2.56	2.73	2.37
	16.7	3.52	2.59	-1.15		17.0	3.47	3.29	.97
	20.1	4.63	3.33	-2.83		20.2	4.39	4.02	-1.06
	23.4	5.59	4.82	-4.60					
(b) M = 3.35									
0	-8.0	-1.41	1.29	1.33	20	-7.8	-1.22	1.44	2.61
	-5.9	-.89	1.25	.82		-5.7	-.69	1.42	2.24
	-2.7	-.43	1.22	.58		-2.5	-.18	1.48	2.08
	.3	-.01	1.32	-.27		.6	.29	1.68	1.94
	.3	-.02	1.27	-.28		.6	.29	1.57	1.88
	3.3	.42	1.18	-1.29		3.7	.76	1.45	1.87
	6.5	.85	1.26	-1.60		6.9	1.08	1.48	2.49
	9.7	1.51	1.40	-1.91		10.1	1.84	1.73	1.06
	12.9	2.48	1.86	-3.02		14.3	2.91	2.42	-.84
	16.1	3.55	2.39	-4.61		16.4	3.54	2.82	-2.16
	19.4	4.70	2.96	-6.39		19.6	4.45	3.60	-4.44
	22.6	5.72	4.00	-8.63		22.7	5.45	4.50	-7.33
10	-7.9	-1.38	1.35	1.95	30	-7.7	-1.02	1.64	3.61
	-5.8	-.86	1.30	1.43		-5.5	-.49	1.67	3.19
	-2.6	-.34	1.32	1.16		-2.3	.07	1.84	3.12
	.4	.10	1.47	.63		.8	.54	1.87	3.44
	.4	.06	1.36	.69		.8	.43	1.86	3.54
	3.5	.41	1.26	.63		4.0	.71	1.76	4.31
	6.6	.89	1.34	.17		7.1	1.03	1.95	4.83
	9.8	1.65	1.55	-.76		10.3	1.61	2.07	4.35
	13.0	2.60	2.04	-2.02		13.5	2.47	2.50	2.49
	16.3	3.57	2.57	-3.59		16.6	3.37	3.18	-.07
	19.5	4.56	3.32	-5.64		19.7	4.30	3.98	-3.25
	22.7	5.66	4.14	-8.26		22.8	5.34	4.75	-6.75

TABLE VI.- EXPERIMENTAL RESULTS FOR MODELS A, B, AND C - TAIL OFF; C.G. AT 0.5001

δ_f, deg	α, deg	C_L	C_D	C_m	δ_f, deg	α, deg	C_L	C_D	C_m
(a) M = 2.44									
0	-8.5	-.70	.89	-2.88	20	-8.4	-.69	1.27	-2.85
	-6.2	-.38	.81	-2.15		-6.1	-.33	1.20	-2.00
	-2.9	-.12	.75	-1.04		-2.8	.01	1.17	-.37
	.4	-.00	.97	.19		.5	.21	1.19	1.28
	.4	.01	.98	.36		.5	.19	1.17	1.33
	3.7	.10	.93	1.45		3.9	.38	1.24	2.97
	7.1	.36	1.02	2.45		7.3	.68	1.34	4.41
	10.4	.84	1.18	3.79		10.7	1.19	1.53	5.05
	13.8	1.61	1.51	5.55		14.1	2.08	1.90	7.68
	17.1	2.65	2.15	5.90		17.5	3.12	2.52	8.58
	20.5	3.90	2.91	5.54		20.8	4.25	3.31	8.05
	23.9	5.17	3.89	4.98		24.2	4.69	3.99	12.80
10	-8.4	-.71	1.17	-2.77	30	-8.2	-.52	1.38	-2.29
	-6.2	-.50	1.11	-2.02		-6.0	-.18	1.36	-1.40
	-2.8	-.08	1.06	-.77		-2.5	.18	1.39	.39
	.5	.04	.06	.27		.8	.43	1.45	2.29
	.5	.03	1.04	.72		.8	.43	1.44	----
	3.8	.16	1.06	1.99		.8	.42	1.43	2.37
	7.2	.42	1.12	3.09		4.2	.66	1.56	4.34
	10.6	.92	1.25	4.50		7.6	.94	1.70	6.28
	14.0	1.78	1.57	6.12		11.0	1.41	1.92	7.71
	17.3	2.81	2.12	6.86		14.4	2.33	2.40	9.43
	20.7	3.98	2.86	6.55		17.8	3.24	3.04	10.35
	24.1	5.17	3.87	6.23		21.3	4.36	3.94	9.89
(b) M = 3.35									
0	-8.1	-.84	1.26	-2.55	20	-7.7	-.78	1.32	-1.88
	-6.0	-.44	1.16	-2.12		-5.6	-.40	1.22	-1.43
	-2.7	-.16	1.09	-1.01		-2.4	-.07	1.19	-.25
	.4	-.02	1.07	-.12		.7	.15	1.23	.99
	.4	-.02	1.08	.01		3.9	.34	1.31	2.47
	3.7	.08	1.10	.91		7.1	.68	1.40	3.89
	6.9	.33	1.19	1.85		10.4	1.25	1.63	5.49
	10.2	.90	1.28	2.81		13.6	2.10	1.97	6.45
	13.4	1.79	1.53	3.39		16.8	2.98	2.48	7.12
	16.7	2.77	1.97	3.32		20.0	3.91	3.14	7.28
	19.9	3.84	2.59	3.44		23.2	4.87	3.99	7.07
	23.2	4.91	3.28	3.87					
10	-7.8	-.82	1.26	-2.32	30	-8.3	.63	-1.20	-1.41
	-5.7	-.55	1.17	-1.84		-5.9	.49	-1.28	-.92
	-2.5	-.13	1.09	-.84		-2.6	-.00	-1.34	.43
	.6	.03	1.12	.19		.6	.40	1.43	2.34
	3.7	.16	1.16	1.32		.6	.39	1.47	2.03
	6.9	.42	1.25	2.35		.6	.38	1.41	----
	10.1	1.00	1.41	3.65		3.9	-.03	1.56	3.74
	13.3	1.86	1.68	4.37		7.2	1.01	1.75	5.64
	16.4	2.80	2.12	4.64		10.6	1.58	2.06	7.56
	19.6	3.80	2.74	5.03		13.9	2.38	2.48	8.76
	22.8	4.84	3.55	5.03		17.2	3.19	3.04	9.32
						20.5	4.01	3.72	8.70

TABLE VII.- EXPERIMENTAL RESULTS FOR MODEL F - M = 3.35

δ_f, deg	α, deg	C_L	C_D	C_m	δ_f, deg	α, deg	C_L	C_D	C_m
(a) c = 0.1001; δ_f = 10°; C.G. at 0.4121									
0	-3.5	-0.24	0.26	-.07	10	-3.4	-0.56	0.22	2.91
	-3.3	-.26	.21	-.01		-3.3	-.56	.26	2.96
	-.2	-.02	.24	-.23		-.2	-.31	.17	2.55
	-.2	.01	.29	-.42		-.1	-.29	.22	2.43
	-.1	-.01	.23	-.29		-.0	-.29	.16	2.44
	2.9	.22	.25	-.54		2.8	-.06	.18	2.07
	2.9	.21	.19	-.47		2.8	-.04	.14	1.97
	9.2	1.05	.53	-1.79		9.3	.82	.30	.70
	15.8	2.74	1.20	-6.49		15.8	2.49	.95	-3.74
	22.6	4.61	2.52	-13.24		22.8	4.33	2.17	-10.16
(b) c = 0.1001; δ_f = 15°; C.G. at 0.4771									
0	-3.3	-.29	.26	.09	15	-3.4	-.79	.52	4.51
	-3.3	-.28	.34	.05		-3.3	-.81	.50	4.55
	-.3	-.01	.24	-.23		-.2	-.51	.45	4.00
	-.0	.00	.33	-.34		-.1	-.51	.42	4.01
	-.0	-.00	.25	-.29		-.1	-.53	.42	4.11
	2.8	.25	.26	-.64		2.8	-.24	.35	3.64
	2.9	.25	.31	-.64		2.9	-.24	.35	3.53
	9.3	1.14	.50	-1.58		9.3	.71	.43	2.89
	15.9	2.94	1.26	-5.37		15.9	2.45	1.06	-1.10
	22.8	4.87	2.70	-10.88		22.8	4.43	2.23	-6.07
(c) c = 0.1001; δ_f = 20°; C.G. at 0.5491									
0	-8.0	-1.36	.81	.81	20	-3.2	-.98	.95	5.22
	-5.9	-.87	.73	.60		-3.1	-.98	.93	5.18
	-2.7	-.38	.69	.21		-.1	-.68	.84	4.85
	.3	-.01	.74	-.24		-.1	-.70	.78	4.90
	.3	-.01	.57	-.24		-.0	-.70	.79	4.89
	.3	-.01	.63	-.17		2.8	-.41	.70	4.60
	.3	-.00	.69	-.21		3.0	-.39	.68	4.48
	3.4	.31	.64	-.63		3.0	-.39	.69	4.45
	6.5	.77	.71	-.91		9.3	.64	.73	3.54
	9.7	1.45	.89	-1.07		16.0	2.57	1.27	1.36
	13.0	2.32	1.22	-1.54		22.8	4.81	2.36	-1.64
	16.3	3.28	1.72	-2.65					
	19.6	4.26	2.41	-4.05					
	22.9	5.26	3.29	-5.65					
(d) c = 0.1832; δ_f = 10°; C.G. at 0.5281									
0	-3.3	-.31	.24	-.14	10	-3.3	-.84	.44	3.51
	-3.3	-.31	.20	-.13		-3.3	-.84	.41	3.53
	-.3	.02	.23	-.30		-.1	-.49	.31	2.94
	-.2	-.00	.16	-.37		-.1	-.49	.43	2.92
	-.2	-.00	.18	-.34		0	-.49	.35	2.88
	2.8	.31	.22	-.73		2.8	-.14	.24	2.29
	2.9	.30	.16	-.69		2.9	-.13	.26	2.24
	9.3	1.33	.49	-1.70		9.3	.90	.43	1.21
	16.0	3.16	1.30	-4.22		16.1	2.81	1.06	-1.49
	23.0	5.12	2.77	-7.80		22.9	4.88	2.30	-4.88

δ_f, deg	α, deg	C_L	C_D	C_m	δ_f, deg	α, deg	C_L	C_D	C_m
(e) c = 0.1831; δ_f = 15°; C.G. at 0.6261									
0	-3.0	-0.38	0.48	-.15	15	-3.1	-1.33	0.97	5.12
	-2.7	-.40	.61	-.06		-3.0	-1.32	.96	5.05
	.1	.01	.46	-.48		.0	-.89	.78	4.47
	.1	.02	.52	-.51		.0	-.90	.84	4.51
	.1	.00	.44	-.47		.2	-.91	.80	4.50
	3.2	.43	.46	-.97		3.0	-.44	.66	3.79
	3.2	.45	.46	-1.02		3.1	-.44	.72	3.75
	9.6	1.69	.78	-1.78		9.5	.78	.78	3.20
	16.4	3.78	1.75	-2.53		15.9	2.99	1.35	1.93
	22.8	5.97	3.34	-3.81		22.7	5.37	2.62	.57
(f) c = 0.2621; δ_f = 10°; C.G. at 0.6251									
0	-8.0	-1.64	.67	-.04	10	-5.7	-1.89	.54	3.59
	-5.9	-1.02	.57	-.31		.4	-.73	.75	2.45
	-2.7	-.43	.46	-.34		.4	-.68	.62	2.33
	.2	-.01	.48	-.39		3.3	-.12	.56	1.54
	.2	.02	.41	-.53		6.5	.42	.65	1.27
	3.3	.50	.44	-1.01		9.7	1.17	.81	1.42
	6.4	1.04	.64	-1.23		12.9	2.27	1.06	1.18
	9.6	1.96	.82	-1.70		16.2	3.46	1.62	.84
	12.8	3.12	1.23	-2.10		19.4	4.63	2.15	-.09
	16.1	4.36	1.85	-2.62					
	19.3	5.67	2.68	-3.34					
	22.6	6.90	3.70	-3.64					
(g) c = 0.2621; δ_f = 15°; C.G. at 0.6791									
0	-3.2	-.70	.96	.64	15	-.1	-1.24	1.13	4.50
	-.4	-.04	1.00	-.27		2.8	-.52	.97	3.29
	2.7	.63	.87	-1.31		2.9	-.52	1.08	3.25
	9.4	2.26	1.25	-2.21		9.2	1.09	1.03	2.31
						15.9	3.85	1.80	1.37
15	-3.3	-1.93	1.32	5.69		22.7	6.61	3.22	1.15
	-3.2	-1.93	1.40	5.75					
	-.1	-1.25	1.23	4.59					
(h) Body alone; C.G. at 0.5281									
0	-3.4	-.19	.05	-.95	0	2.9	.17	.05	.39
	-3.4	-.21	.04	-.91		6.0	.44	.11	1.01
	-.2	-.02	.03	-.20		9.4	.96	.23	1.39
	-.1	-.00	.05	-.27		12.6	1.72	.49	1.45
	-.1	-.02	.03	-.19		16.1	2.52	.86	1.47
	2.7	.16	.06	.43		19.5	3.35	1.37	1.09
						22.9	4.17	2.05	.62

TABLE VIII.- EXPERIMENTAL RESULTS FOR MODEL G; C.G. AT 0.585$\bar{c}$

(a) M = 1.76

δ_f, deg	α, deg	C_L	C_D	C_m
0	-6.1	-0.78	0.67	1.61
	-3.1	-.40	.63	.98
	-1.1	-.14	.63	.41
	0	.02	.63	.09
	.8	.14	.64	-.21
	2.9	.43	.67	-.80
	5.8	.82	.76	-1.37
	8.8	1.34	.86	-1.90
	11.8	1.90	1.01	-2.15
	14.9	2.62	1.28	-1.73
	17.9	3.69	1.75	-.72
	20.9	4.77	2.37	.04
	21.8	5.27	2.61	.07
	22.9	5.81	2.93	-.15
	23.9	6.49	3.30	-1.10
6	-6.1	-1.05	.84	3.28
	-3.0	-.65	.73	2.56
	-1.2	-.39	.69	1.95
	0	-.22	.68	1.56
	.8	-.15	.67	1.36
	2.8	.12	.68	.85
	5.8	.51	.74	.32
	9.0	1.06	.83	-.19
	11.8	1.61	.95	-.45
	14.9	2.37	1.20	-.17
	17.8	3.41	1.63	.68
	20.9	4.64	2.26	1.32
	22.3	5.27	2.61	1.58
	24.0	6.30	3.16	.49
12	-6.1	-1.33	1.02	5.32
	-3.2	-.95	.89	4.57
	-1.2	-.66	.82	3.86
	0	-.56	.79	3.61
	.8	-.42	.77	3.23
	2.7	-.16	.76	2.66
	5.7	.24	.78	2.10
	8.9	.73	.87	1.76
	11.8	1.28	.99	1.53
	14.9	2.09	1.22	1.81
	17.9	3.12	1.62	2.61
	20.9	4.35	2.21	3.08
	21.9	4.72	2.42	3.41
	22.9	5.25	2.71	3.20
	23.8	5.97	3.02	2.41
17	-6.1	-1.62	1.20	7.16
	-3.1	-1.23	1.05	6.37
	-1.1	-1.01	.94	5.82
	.1	-.86	.88	5.42
	.9	-.75	.85	5.12
	2.8	-.46	.80	4.45
	5.9	-.04	.80	3.72
	8.8	.44	.86	3.32
	11.8	1.02	.98	3.01
	14.9	1.81	1.22	3.14
	17.9	2.90	1.63	3.80
	19.3	3.48	1.87	3.97
	20.9	4.17	2.17	4.15
	22.5	4.93	2.54	4.11
	23.9	5.86	2.95	3.18

(b) M = 2.00

δ_f, deg	α, deg	C_L	C_D	C_m
0	-6.2	-.74	.60	1.23
	-3.1	-.40	.56	.97
	-1.1	-.15	.55	.55
	0	-.00	.55	.31
	.9	.13	.56	.04
	2.8	.41	.58	-.49
	5.8	.87	.66	-1.07
	8.9	1.42	.78	-1.48
	11.8	2.06	.95	-1.10
	14.9	2.97	1.31	-.32
	17.8	4.00	1.80	-.06
	20.9	5.10	2.44	-.24
	23.9	6.43	3.33	-1.22
6	-6.1	-.99	.75	2.93
	-3.1	-.63	.67	2.51
	-1.2	-.38	.62	2.07
	0	-.22	.60	1.75
	.7	-.11	.60	1.53
	2.8	.16	.60	1.01
	5.9	.58	.66	.63
	8.9	1.11	.72	.29
	11.8	1.81	.89	.60
	14.9	2.71	1.21	1.30
	17.8	3.76	1.67	1.61
	20.9	4.80	2.24	1.65
	23.9	6.28	3.15	.31
12	-6.0	-1.29	.96	5.03
	-3.0	-.90	.83	4.42
	-1.2	-.68	.76	4.00
	0	-.47	.72	3.57
	.8	-.40	.71	3.36
	2.8	-.12	.69	2.85
	5.8	.25	.71	2.49
	8.9	.82	.78	2.08
	11.9	1.54	.94	2.32
	14.9	2.45	1.21	3.07
	16.6	3.01	1.43	3.28
	17.8	3.49	1.63	3.25
	20.9	4.64	2.22	3.06
	22.9	5.49	2.73	2.50
	24.0	6.04	3.04	1.90
17	-6.1	-1.55	1.11	6.80
	-3.0	-1.21	.99	6.27
	-1.1	-.97	.90	5.81
	0	-.85	.85	5.55
	1.0	-.70	.81	5.18
	2.9	-.45	.77	4.72
	5.9	-.03	.75	4.18
	8.9	.48	.79	3.87
	11.8	1.29	.96	3.79
	14.8	2.17	1.22	4.33
	17.8	3.28	1.62	4.32
	19.3	3.80	1.85	4.27
	20.9	4.47	2.18	3.96
	22.5	5.11	2.53	3.57
	23.9	5.87	2.92	2.82

(c) M = 2.20

δ_f, deg	α, deg	C_L	C_D	C_m
0	-6.1	-0.67	.66	.76
	-3.0	-.31	.60	.39
	-1.2	-.08	.58	.10
	0	.07	.59	-.20
	.8	.23	.58	-.42
	2.8	.46	.60	-.71
	5.8	.86	.66	-1.04
	8.8	1.43	.77	-1.36
	11.8	2.17	1.00	-.79
	14.9	3.06	1.36	-.18
	17.8	4.13	1.86	-.26
	20.9	5.16	2.51	-.70
	23.7	6.49	3.38	-1.99
6	-6.1	-.95	.78	2.51
	-3.0	-.58	.70	2.03
	-1.2	-.30	.65	1.62
	0	-.18	.62	1.41
	.8	-.06	.61	1.22
	2.8	.13	.61	1.03
	5.9	.56	.66	.70
	8.8	1.19	---	.53
	11.8	1.89	.91	.93
	14.9	2.78	1.25	1.55
	17.9	3.84	1.74	1.48
	20.9	4.95	2.35	.98
	23.9	6.38	3.24	-.56
12	-6.1	-1.21	1.03	4.53
	-3.0	-.83	.89	3.95
	-1.0	-.62	.80	3.60
12	0	-.48	.75	3.32
	1.0	-.37	.73	3.10
	2.8	-.16	.71	2.83
	5.8	.27	.73	2.47
	9.0	.81	.77	2.35
	11.9	1.61	.96	2.75
	14.9	2.51	1.24	3.29
	16.4	3.02	1.43	2.67
	17.9	3.62	1.69	3.14
	20.9	4.64	2.24	2.78
	22.9	5.58	2.76	1.92
	24.0	6.16	3.08	.96
17	-6.1	-1.42	1.18	6.09
	-3.0	-1.10	1.04	5.61
	-1.2	-.83	.94	5.08
	.1	-.75	.89	4.94
	.8	-.61	.87	4.66
	3.0	-.33	.81	4.22
	5.9	-.00	.80	3.99
	8.9	.54	.83	3.77
	11.9	1.35	1.01	4.09
	14.9	2.28	1.27	4.41
	17.9	3.35	1.68	4.18
	19.4	3.94	1.94	3.86
	20.9	4.57	2.25	3.47
	22.5	5.23	2.61	2.95
	23.9	5.96	2.96	1.85

(d) M = 3.00

δ_f, deg	α, deg	C_L	C_D	C_m
0	-3.0	-.43	.53	.82
	-1.0	-.15	.49	.35
	0	-.01	.49	.14
	0	-.01	.48	.12
	0	-.01	.49	.11
	1.0	.11	.49	-.09
	2.0	.23	.51	-.27
	4.0	.50	.55	-.64
	7.0	.98	.65	-.53
	8.1	1.20	.70	-.58
	10.2	1.70	.84	-.31
	10.2	1.70	.83	-.34
	10.2	1.73	.85	-.35
	11.3	1.98	.92	-.30
	12.4	2.28	1.03	-.39
6	-3.1	-.73	.63	2.75
	-1.0	-.46	.63	2.26
	-.0	-.33	.54	2.03
	-.0	-.33	.54	2.03
	-.0	-.33	.54	2.02
	.9	-.20	.53	1.78
	2.0	-.06	.53	1.53
	4.0	.19	.54	1.15
	7.0	.64	.58	1.66
	8.1	.85	.62	1.68
	10.2	1.36	.74	1.83
	10.2	1.35	.74	1.78
	10.2	1.36	.74	1.77
	12.3	1.94	.90	1.77
12	-3.1	-1.00	.94	4.47
	-1.0	-.74	.84	4.00
	-.0	-.61	.80	3.74
12	-.0	-.59	.78	3.66
	-.0	-.61	.80	4.40
	.9	-.48	.78	3.51
	1.9	-.35	.75	3.25
	4.0	-.07	.73	2.72
	7.0	.35	.63	3.41
	8.0	.55	.66	3.47
	10.2	1.07	.76	3.56
	10.2	1.07	.75	3.56
	10.2	1.08	.76	3.57
	12.3	1.68	.88	3.39
17	-3.1	-1.22	.95	7.91
	-1.1	-.97	.84	7.01
	-.0	-.85	.79	6.62
	-.0	-.85	.78	6.54
	-.0	-.85	.78	6.52
	.9	-.73	.74	6.12
	1.9	-.60	.70	5.65
	4.0	-.32	.66	4.71
	6.9	.08	.72	4.70
	8.0	.27	.74	4.46
	10.1	.80	.85	3.66
	10.1	.79	.84	3.64
	10.1	.80	.84	3.60
	12.3	1.41	.95	2.49
	12.3	1.40	1.05	1.81
	13.4	1.72	1.10	1.09
	15.6	2.43	1.20	-.69
	15.6	2.43	1.19	-.68
	15.6	2.48	1.22	-.81

[redacted]

TABLE VIII.- EXPERIMENTAL RESULTS FOR MODEL G; C.G. AT 0.5831 - CONCLUDED

δ_f, deg	α, deg	C_L	C_D	C_m	δ_f, deg	α, deg	C_L	C_D	C_m	δ_f, deg	α, deg	C_L	C_D	C_m	δ_f, deg	α, deg	C_L	C_D	C_m
(e) M = 4.24										(f) M = 5.05									
0	-3.0	-.51	.57	1.22	12	-3.0	-1.00	.88	4.23	0	-3.0	-.49	.50	.92	12	-3.0	-1.08	.82	4.04
	-1.0	-.21	.53	.72		-1.0	-.74	.80	3.96		-1.0	-.19	.48	.51		-1.0	-.73	.74	3.74
	-.0	-.08	.53	.53		-.0	-.61	.76	3.75		0	-.03	.48	.29		-.0	-.57	.70	3.48
	-.0	-.07	.53	.45		-.0	-.60	.75	3.72		0	-.04	.48	.26		-.0	-.58	.70	3.49
	0	-.04	.51	.32		-.0	-.62	.75	3.83		0	-.03	.48	.23		-.0	-.58	.71	3.50
	1.0	.07	.53	.03		.9	-.46	.71	3.44		1.0	.13	.48	-.13		.9	-.44	.66	3.28
	2.0	.23	.53	-.10		2.0	-.32	.71	3.22		2.0	.28	.49	-.32		2.0	-.28	.63	3.00
	4.0	.53	.55	-.34		4.0	-.03	.64	2.87		4.0	.57	.51	-.55		4.0	-.03	.59	2.53
	6.9	1.08	.69	-.21		6.9	.48	.63	4.04		6.9	1.04	.68	-.07		6.9	.53	.58	3.25
	8.0	1.35	.74	-.42		7.9	.74	.66	3.44		7.9	1.35	.74	-.65		7.9	.81	.62	2.84
	10.0	1.85	.91	-.56		10.0	1.28	.74	3.15		9.9	1.80	.91	-.90		9.9	1.32	.69	2.30
	10.0	1.85	.90	-.55		10.0	1.27	.73	3.17		9.9	1.85	.92	-1.14		9.9	1.32	.70	2.39
	10.0	1.85	.90	-.56		10.0	1.28	.72	3.14		9.9	1.87	.95	-1.17		9.9	1.33	.70	2.33
	12.1	2.40	1.13	-.97		12.1	1.84	.88	2.74		12.0	2.38	1.13	-1.70		12.0	1.83	.86	1.96
	12.2	2.44	1.14	-1.84		12.1	1.78	.83	2.68		12.0	2.41	1.17	-2.43		12.0	1.80	.79	1.60
	13.2	2.72	1.26	-2.18		13.2	2.06	.93	2.47		13.0	2.76	1.29	-2.66		13.0	2.07	.90	1.26
	15.3	3.31	1.58	-2.84		15.3	2.72	1.22	1.41		15.1	3.23	1.61	-3.60		15.0	2.62	1.17	.74
	15.3	3.34	1.60	-2.90		15.3	2.69	1.20	1.70		15.1	3.23	1.62	-3.43		15.1	2.65	1.17	.58
	15.3	3.33	1.58	-2.93		15.3	2.71	1.52	1.53		15.1	3.26	1.63	-3.45		15.1	2.64	1.16	.50
	17.4	3.92	1.94	-4.38		17.3	3.25	1.22	1.37		17.1	3.80	1.97	-3.96		17.1	3.14	1.44	.14
6	-3.0	-.76	.64	2.63	17	-3.0	-1.23	1.00	5.76	6	-3.0	-.77	.61	2.58	17	-3.0	-1.21	.95	5.68
	-1.0	-.49	.58	2.35		-1.0	-.98	.88	5.50		-1.0	-.49	.56	2.25		-1.0	-.96	.85	5.49
	-.0	-.34	.55	2.10		-.0	-.85	.82	5.30		-.0	-.33	.52	2.03		-.0	-.80	.79	5.02
	-.0	-.34	.55	2.12		-.0	-.85	.83	5.28		-.0	-.34	.53	2.04		-.0	-.82	.80	5.38
	-.0	-.33	.55	2.10		-.0	-.84	.83	5.22		-.0	-.34	.53	2.02		-.0	-.82	.80	5.73
	1.0	-.19	.53	1.83		.9	-.72	.78	5.08		1.0	-.18	.51	1.72		.9	-.67	.75	4.92
	2.0	-.05	.52	1.60		1.9	-.57	.73	4.79		2.0	-.02	.49	1.46		1.9	-.52	.70	4.76
	4.0	.26	.53	1.10		4.0	-.27	.68	4.38		4.0	.28	.48	1.02		4.0	-.20	.64	4.18
	6.9	.57	.65	2.20		6.9	.26	.74	4.86		6.9	.81	.57	1.58		6.9	.36	.68	4.38
	8.0	1.04	.65	1.68		7.9	.49	.75	4.88		7.9	1.09	.60	1.12		7.9	.59	.72	4.21
	10.0	1.56	.76	1.38		10.0	1.05	.80	4.51		9.9	1.56	.74	.79		9.9	1.10	.73	3.72
	10.0	1.57	.77	1.42		10.0	1.04	.80	4.53		9.9	1.44	1.51	.76		9.9	1.11	.75	3.78
	10.0	1.57	.77	1.45		10.0	1.04	.81	4.55		9.9	1.58	.75	.76		9.9	1.13	.73	3.80
	12.1	2.12	.96	.12		12.1	1.63	.90	3.96		12.0	2.08	.93	.38		11.9	1.65	.85	3.31
	12.2	2.10	.92	.34		12.1	1.62	.90	2.88		12.0	2.01	.90	0		12.0	1.65	.82	2.26
	13.2	2.39	1.04	.07		13.2	1.92	.96	2.59		13.0	2.37	1.07	-.70		13.0	1.92	.99	1.97
	15.3	3.05	1.37	-.85		15.2	2.53	1.27	1.73		15.1	2.84	1.34	-1.04		15.1	2.43	1.25	1.22
	15.3	3.01	1.33	-.79		15.2	2.52	1.26	1.78		15.1	2.94	1.33	-1.37		15.1	2.45	1.24	1.47
	15.3	3.01	1.35	-.85		15.2	2.51	1.32	1.86		15.1	2.95	1.34	-1.32		15.1	2.48	1.24	1.42
	17.4	3.63	1.67	-1.37		17.4	3.12	1.52	1.35		17.1	3.48	1.64	-2.22		17.1	2.99	1.48	1.10

TABLE IX.- EXPERIMENTAL RESULTS FOR MODEL G AT SEVERAL ROLL ANGLES - M = 2.00; C.G. AT 0.585$\bar{c}$

(a) φ = 0°, δ = 0°

α, deg	C_L	C_D	C_m	C_l	C_Y	C_n
-6.2	-0.74	0.60	1.23	0.01	0.07	-.20
-3.1	-.40	.56	.97	.01	.07	-.19
-1.1	-.15	.55	.53	.01	.06	-.19
0	-.00	.55	.31	.01	.06	-.19
.9	.13	.56	.04	.01	.06	-.18
2.8	.41	.58	-.49	.01	.06	-.18
5.8	.87	.66	-1.07	.01	.09	-.15
8.9	1.42	.78	-1.48	.01	.08	-.09
11.8	2.06	.95	-1.10	.01	.02	-.05
14.9	2.97	1.31	-.32	.01	.05	-.13
17.8	4.00	1.80	-.06	.01	.15	-.39
20.9	5.10	2.44	-.24	.02	.28	-.73
23.9	6.43	3.33	-1.22	.02	-.25	.22

(b) φ = 22.5°, δ = 0°

α, deg	C_L	C_D	C_m	C_l	C_Y	C_n
-6.1	-0.66	0.71	1.23	-0.01	-0.01	-.13
-6.2	-.66	.71	1.23	-.00	-.01	-.13
-3.1	-.33	.66	.96	.00	-.01	-.04
-1.1	-.17	.64	.68	-.00	-.01	-.04
-1.1	-.17	.60	.68	-.00	-.02	-.02
.1	-.00	.59	.32	-.00	-.01	-.04
.8	.15	.59	-.01	-.00	-.02	0
.9	.18	.58	.08	-.00	-.02	0
2.9	.38	.60	-.44	-.00	-.04	.07
5.9	.82	.68	-.97	-.01	-.04	.16
8.9	1.35	.78	-1.31	-.03	-.04	.22
11.8	2.10	1.00	-1.09	-.03	-.06	.23
14.9	2.91	1.33	-.28	-.01	-.06	.21
17.9	3.98	1.83	-.13	-.01	-.10	.10
21.0	5.12	2.48	-.49	-.03	-.11	-.09
20.9	5.11	2.47	-.46	-.03	-.10	-.11
23.9	6.42	3.35	-1.29	-.03	-.09	.64

(c) φ = 45°, δ = 0°

α, deg	C_L	C_D	C_m	C_l	C_Y	C_n
-6.3	-0.70	0.79	1.20	0.00	-0.04	.02
-3.1	-.35	.68	.83	-.00	-.03	.01
-1.1	-.09	.62	.42	-.00	-.04	.02
.1	.07	.60	.08	-.00	-.03	.03
1.1	.17	.60	-.10	-.00	-.03	.02
2.9	.38	.60	-.44	-.00	-.02	.01
5.9	.88	.67	-1.19	-.00	-.02	0
9.0	1.41	.79	-1.46	-.01	-.01	0
11.8	2.05	.98	-1.15	-.01	-.02	.01
14.8	2.92	1.31	-.57	-.00	.00	0
17.9	4.05	1.83	-.49	.00	.00	.01
19.4	4.57	2.13	-.59	.00	.00	.05
20.9	5.19	2.51	-.85	-.00	.02	.19
22.6	5.85	2.97	-1.29	-.01	-.01	.80
23.9	6.51	3.43	-1.91	-.01	-.10	1.61

(d) φ = 67.5°, δ = 0°

α, deg	C_L	C_D	C_m	C_l	C_Y	C_n
-6.3	-.64	.86	1.10	-.01	-.04	.07
-3.2	-.37	.73	.93	-.01	-.04	.03
-1.1	-.13	.69	.53	-.01	-.04	.02
-.1	-.02	.66	.28	-.01	-.03	.03
.8	.13	.65	-.03	-.01	-.03	.02
2.9	.42	.66	-.97	-.01	-.02	-.02
5.9	.84	.73	-1.07	-.00	-.01	-.09
8.9	1.42	.84	-1.54	.00	.00	-.13
12.0	2.12	1.06	-1.15	.00	.03	-.18
15.0	2.92	1.38	-.46	-.00	-.01	-.12
17.8	3.94	1.84	-.24	-.00	.02	-.15
19.3	4.47	2.13	-.22	—	.04	-.09
21.0	5.13	2.58	-.55	.00	.06	.06
22.6	5.81	2.97	-1.00	-.00	.03	.78
24.0	6.48	3.42	-1.73	-.00	-.03	1.51

(e) φ = 0°, δ = 17°

α, deg	C_L	C_D	C_m	C_l	C_Y	C_n
-6.1	-1.55	1.11	6.80	.00	.03	-.02
-3.0	-1.21	.99	6.27	.00	.03	-.02
-1.1	-.97	.90	5.81	.00	.03	-.04
0	-.85	.85	5.55	.00	.04	-.07
1.0	-.70	.81	5.18	.00	.04	-.07
2.9	-.45	.77	4.72	.00	.03	-.07
5.9	-.03	.75	4.18	.00	.02	-.04
8.9	.48	.79	3.87	.00	.04	-.12
11.8	1.29	.96	3.79	.00	.03	-.11
14.8	2.17	1.22	4.33	.00	.06	-.19
17.8	3.85	1.62	4.32	.01	.14	-.44
19.3	3.80	1.85	4.27	.03	.15	-.44
20.9	4.47	2.18	3.96	.03	.14	-.30
22.5	5.11	2.53	3.57	.02	.03	.15
23.9	5.87	2.92	2.82	-.00	.02	-.28

(f) φ = 45°, δ = 17°

α, deg	C_L	C_D	C_m	C_l	C_Y	C_n
-6.1	-1.36	1.22	5.60	.07	-.50	3.05
-3.1	-.97	1.05	4.84	.02	-.35	3.36
-1.1	-.71	.94	4.27	-.01	-.37	3.49
0	-.57	.89	3.96	-.03	-.38	3.53
.8	-.46	.85	3.68	-.03	-.38	3.55
2.9	-.20	.79	3.12	-.07	-.36	3.43
5.9	.26	.79	2.46	-.14	-.33	3.20
8.9	.78	.79	2.21	-.23	-.18	2.95
12.0	1.47	.91	2.72	-.28	-.40	2.45
14.8	2.29	1.15	3.36	-.33	-.34	2.04
17.8	3.37	1.57	3.70	-.38	-.34	1.68
19.3	3.90	1.81	3.70	-.41	-.31	1.48
20.9	4.45	2.11	3.66	-.44	-.26	1.26
22.5	5.15	2.52	2.40	-.48	-.22	1.18
24.1	5.84	2.99	3.12	-.52	-.22	1.53

(g) φ = 90°, δ = 17°

α, deg	C_L	C_D	C_m	C_l	C_Y	C_n
-6.1	-.82	1.10	2.01	.14	-.86	5.24
-3.0	-.48	.97	1.48	.07	-.84	5.16
-1.1	-.20	.90	.82	.01	-.83	5.13
0	-.05	.89	.42	-.01	-.83	5.12
.9	.11	.88	.02	-.04	-.83	5.11
2.8	.40	.91	-.64	-.11	-.84	5.16
5.9	.88	1.00	-1.47	-.22	-.86	5.25
8.8	1.45	1.11	-2.15	-.33	-.88	5.36
11.8	2.16	1.32	-2.13	-.44	-.87	5.37
14.8	3.08	1.56	-1.58	-.53	-.86	5.27
17.8	4.11	2.14	-1.49	-.62	-.78	5.16
19.3	4.61	2.43	-1.52	—	-.73	5.26
20.9	5.23	2.80	-1.77	-.72	-.71	5.63
22.5	5.98	3.24	-2.31	-.79	-.80	6.75
23.9	6.65	3.72	-3.20	-.88	-.92	7.76

(h) φ = 135°, δ = 17°

α, deg	C_L	C_D	C_m	C_l	C_Y	C_n
-6.3	-.18	.84	-1.93	.11	-.55	3.39
-3.2	.20	.88	-2.44	.04	-.60	3.63
-1.1	.50	.91	-3.12	.00	-.61	3.68
0	.62	.93	-3.47	-.02	-.60	3.66
.9	.73	.95	-3.74	-.03	-.59	3.61
2.9	1.03	1.02	-4.43	-.07	-.55	3.42
5.9	1.51	1.17	-5.38	-.13	-.50	3.12
8.9	2.06	1.36	-6.03	-.19	-.44	2.83
11.9	2.73	1.62	-5.99	-.25	-.39	2.55
14.9	3.61	2.02	-5.60	-.32	-.35	2.24
17.9	4.69	2.61	-5.78	-.40	-.32	1.87
19.4	5.21	2.96	-6.02	-.44	-.30	1.65
21.0	5.82	3.40	-6.45	-.49	-.26	1.34
22.4	6.43	3.88	-6.91	-.54	-.21	1.12
23.9	7.05	4.41	-7.47	-.59	-.17	1.23

(i) φ = 180°, δ = 17°

α, deg	C_L	C_D	C_m	C_l	C_Y	C_n
-6.2	.12	.78	-3.68	.00	-.03	.11
-3.1	.52	.78	-4.15	-.00	-.03	.11
-1.1	.73	.87	-4.63	.00	-.04	.13
.1	.91	.90	-5.08	.00	-.04	.13
.9	1.02	.93	-5.34	.00	-.05	.15
3.0	1.28	1.04	-5.92	-.00	-.04	.16
6.0	1.64	1.19	-6.39	-.00	-.04	.18
9.1	2.17	1.41	-6.77	-.00	-.04	.18
11.9	2.74	1.66	-6.36	-.01	-.03	.20
14.9	3.58	2.05	-5.60	.00	-.03	.16
17.9	4.55	2.64	-5.27	.00	-.04	.21
19.2	5.01	2.94	-5.30	.00	-.04	.20
20.9	5.57	3.35	-5.44	-.00	-.04	.20
22.6	6.23	3.89	-5.93	.05	-.04	.16
24.0	6.81	4.39	-6.28	-.01	-.05	.04

(j) φ = 90°, δ = 6°

α, deg	C_L	C_D	C_m	C_l	C_Y	C_n
-6.2	-0.73	0.75	1.37	0.06	-0.88	1.63
-3.2	-.41	.69	1.11	.03	-.28	1.57
-1.1	-.15	.63	.61	-.00	-.26	1.51
0	.03	.63	.24	-.00	-.27	1.52
.9	.13	.64	.06	-.02	-.27	1.51
3.0	.38	.67	-.42	-.06	-.27	1.57
6.0	.83	.74	-1.02	-.10	-.29	1.67
8.9	1.34	.83	-1.40	-.15	-.30	1.77
12.1	2.14	1.06	-1.25	-.19	-.31	1.88
14.9	2.97	1.38	-.69	-.22	-.30	1.82
17.9	3.99	1.88	-.38	-.24	-.30	1.82
19.4	4.50	2.16	-.36	-.25	-.27	1.80
20.9	5.10	2.51	-.64	-.26	-.23	1.92
22.5	5.81	2.97	-1.14	-.29	-.28	2.84
24.0	6.52	3.45	-1.94	-.32	-.39	3.85

(k) φ = 90°, δ = 12°

α, deg	C_L	C_D	C_m	C_l	C_Y	C_n
-6.1	-0.74	0.90	1.56	0.11	-0.60	3.57
-3.2	-.38	.81	1.12	.05	-.59	3.49
-1.1	-.08	.77	.51	.00	-.57	3.44
0	-.01	.77	.34	-.02	-.57	3.44
.9	.15	.77	-.06	-.04	-.56	3.42
3.0	.42	.79	-.58	-.11	-.58	3.49
5.9	.84	.87	-1.18	-.18	-.59	3.58
8.9	1.42	.98	-1.80	-.27	-.63	3.73
12.0	2.17	1.19	-1.70	-.35	-.63	3.80
14.9	3.02	1.53	-1.09	-.42	-.63	3.77
17.9	4.05	2.03	-.87	-.48	-.60	3.69
19.3	4.58	2.28	-.85	-.51	-.57	3.64
20.9	5.12	2.54	-1.10	-.53	-.52	3.83
22.6	5.89	3.14	-1.70	-.59	-.59	4.81
23.9	6.53	3.57	-2.41	-.64	-.72	5.86

[redacted]

[redacted]

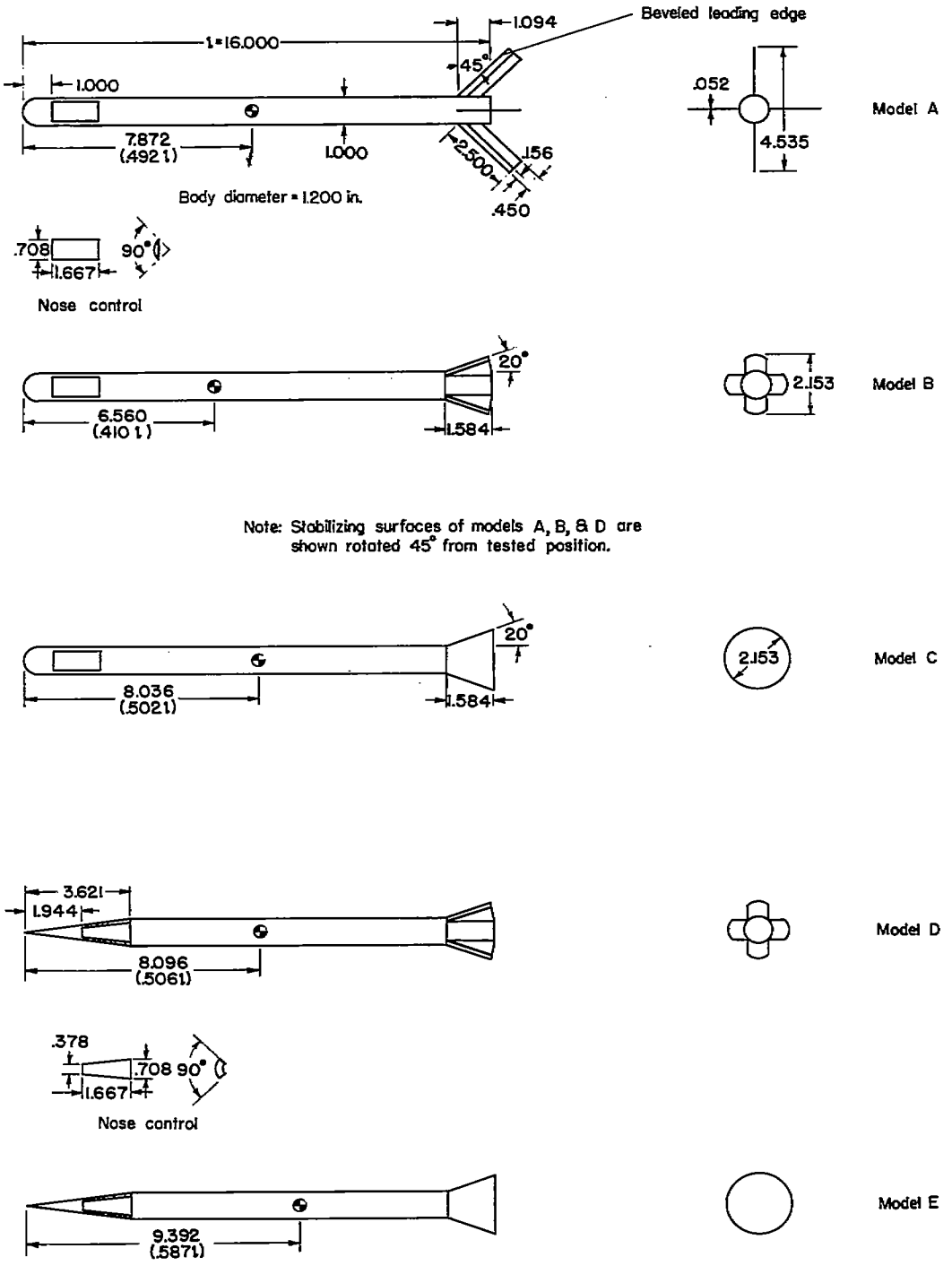

Figure 1.- Sketches of models for first phase of investigation; dimensions in body diameters.

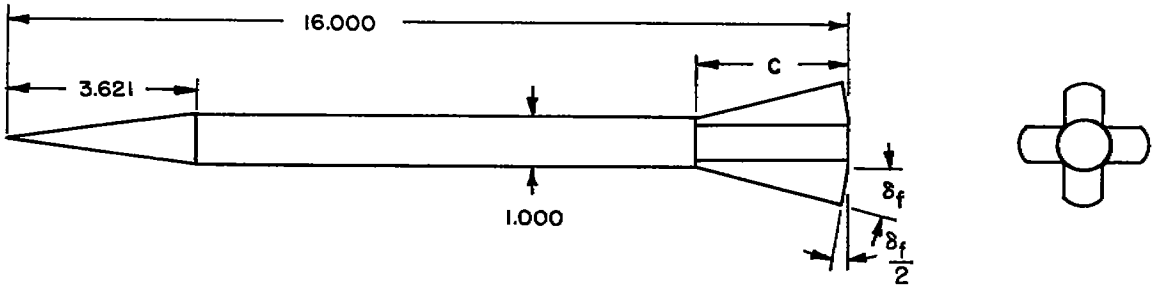

Body diameter = 1.200 in.

c, percent l	δ_f, deg	c.g. position, percent l
10.0	10	41.2
	15	47.7
	20	54.9
18.3	10	52.8
	15	62.6
26.2	10	62.5
	15	67.9

Figure 2.- Sketch of model for second phase of investigation (model F); dimensions in body diameters.

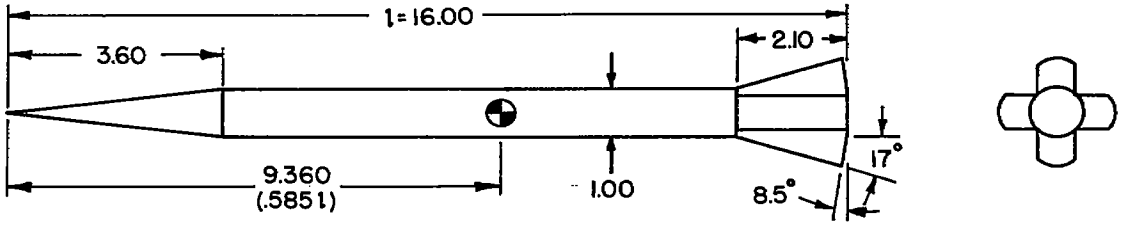

Note: Dimensions in body diameters

6- by 6-foot wind tunnel model	3.600 in.
10- by 14-inch wind tunnel model	1.000 in.

Figure 3.- Sketch of model for third phase of investigation (model G).

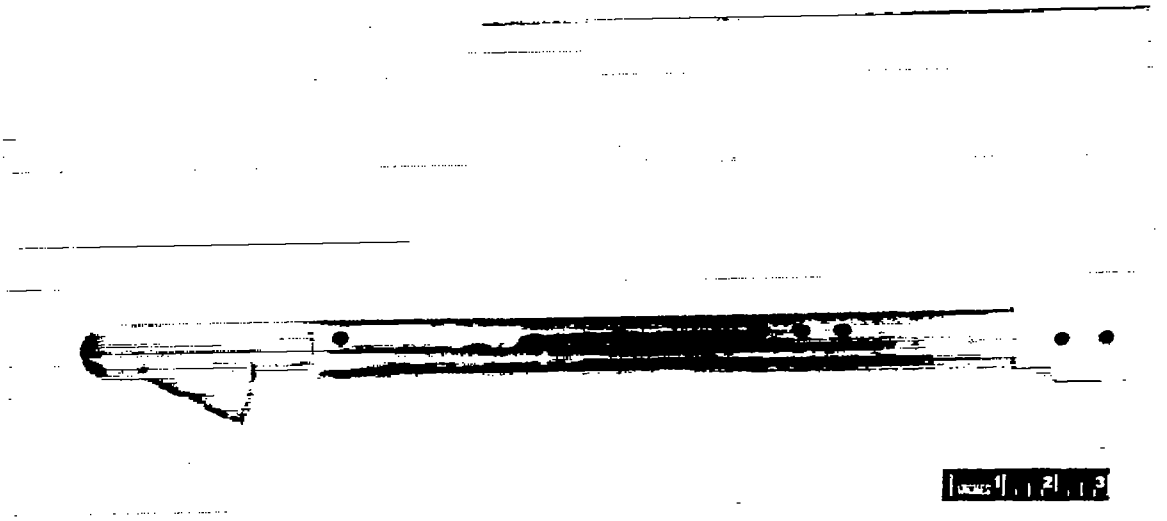

A-21356

(a) Model C

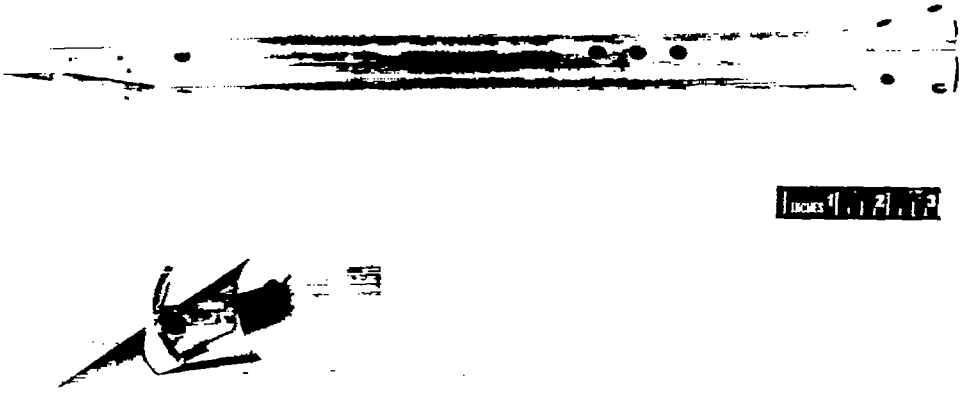

A-21355.1

(b) Model D

Figure 4.- Photographs of models.

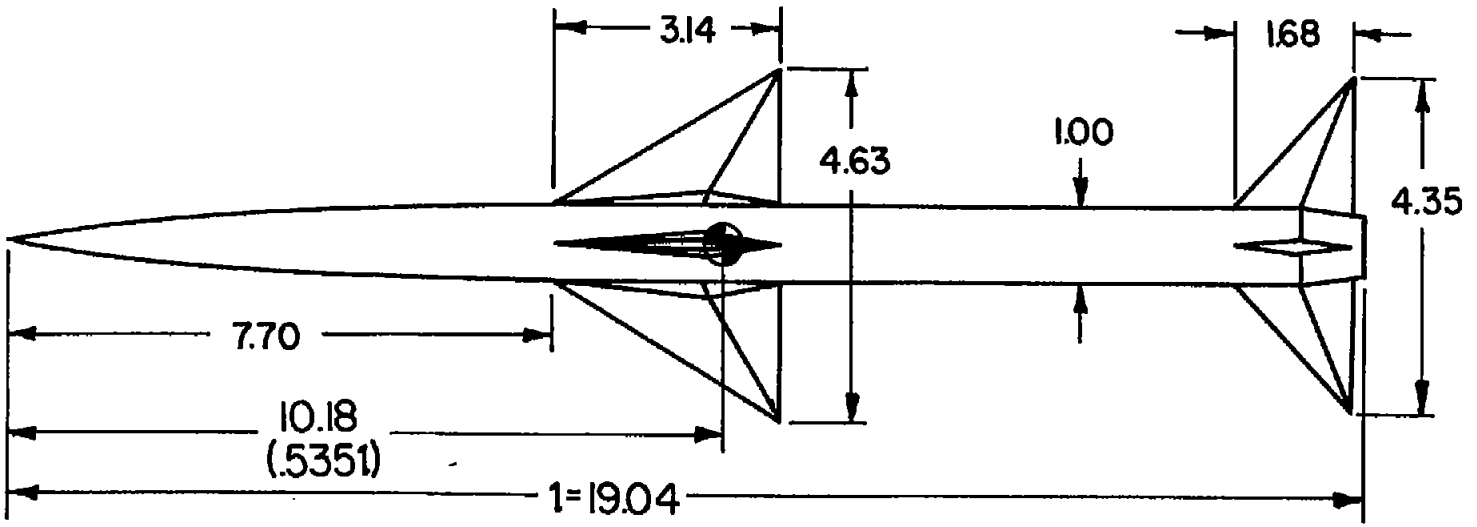

Figure 5.- Sketch of cruciform missile; dimensions in body diameters.

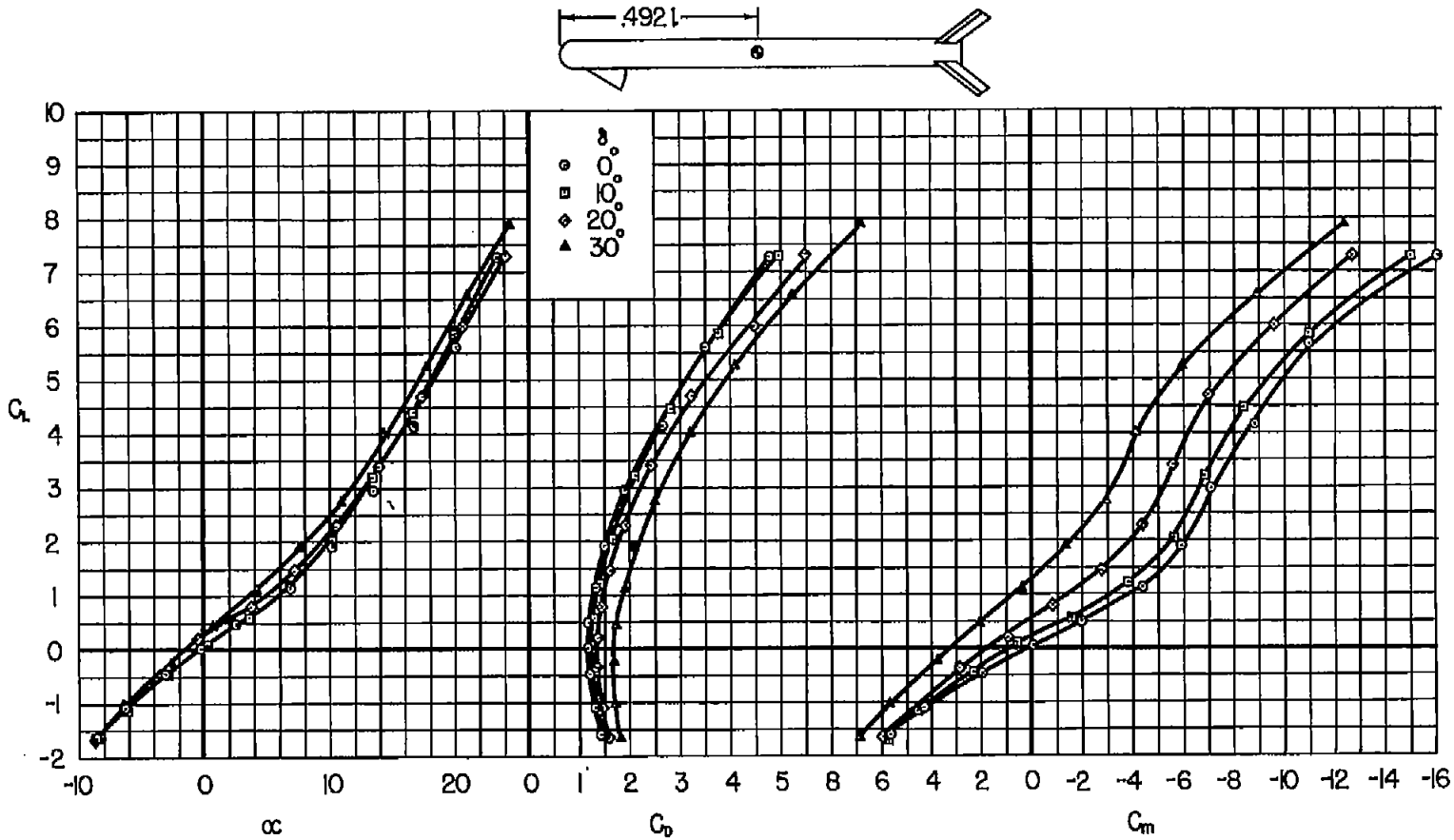

(a) M = 2.44

Figure 6.- Lift, drag, and pitching-moment characteristics of model A.

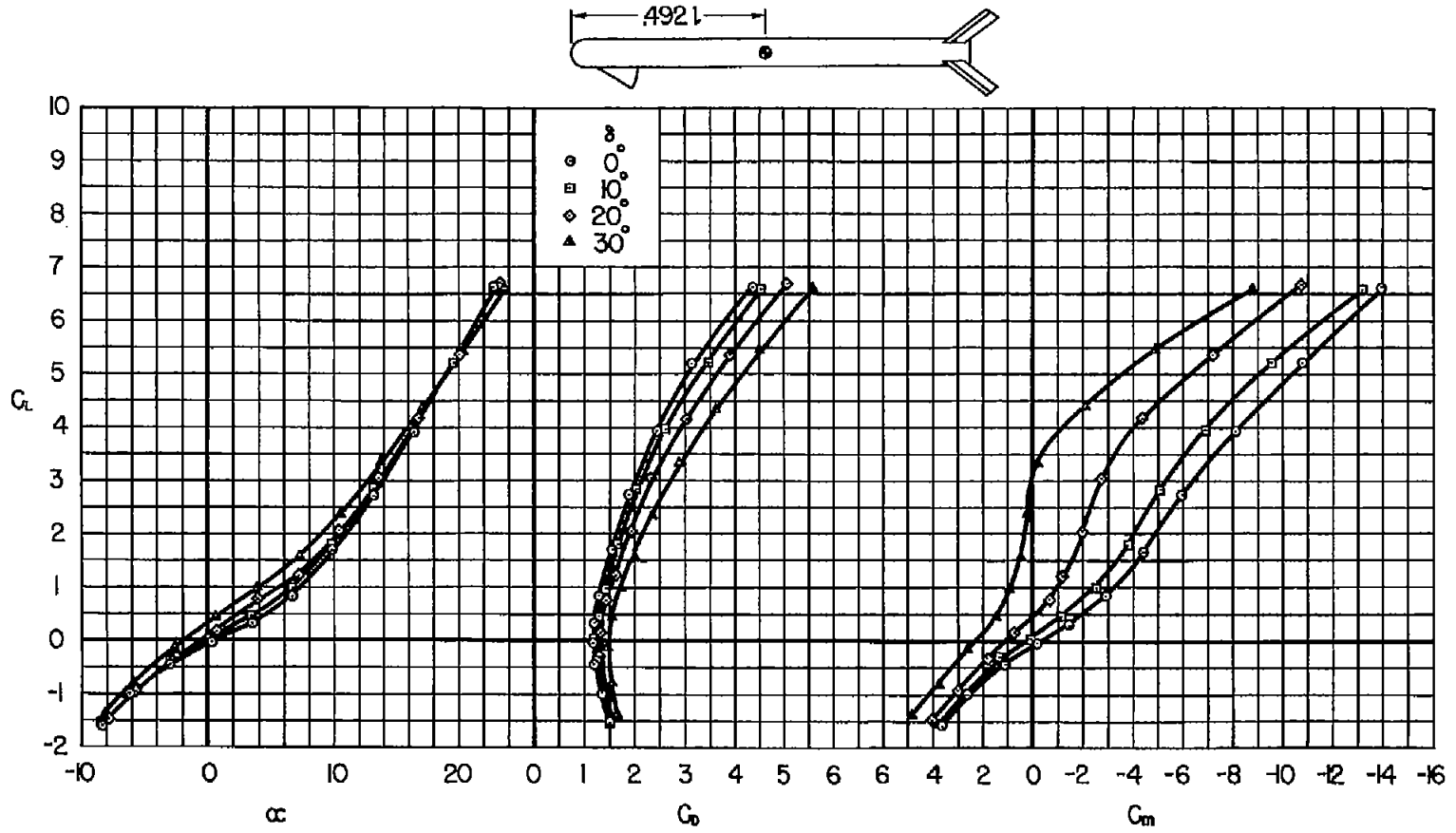

(b) M = 3.35

Figure 6.- Concluded.

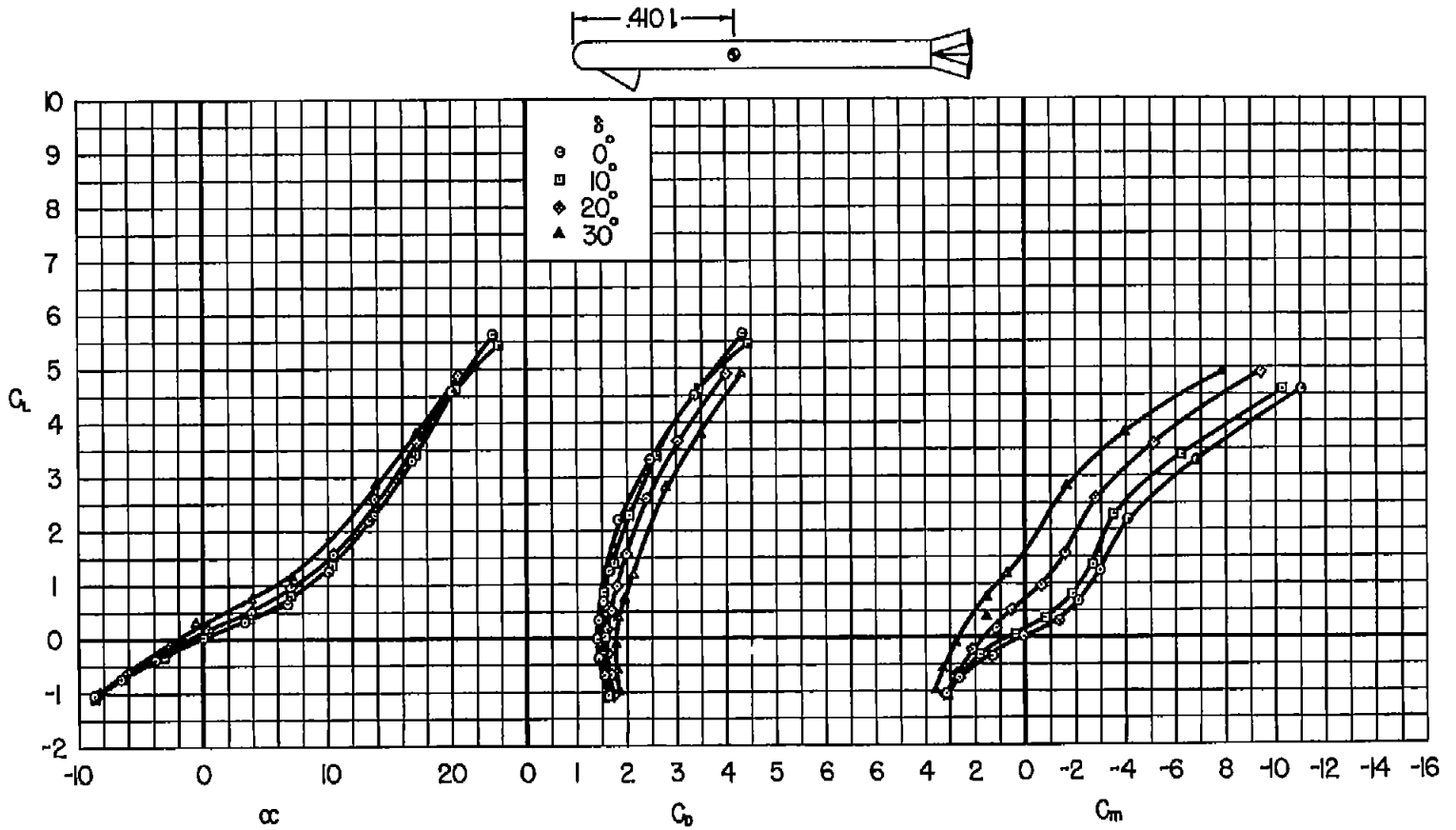

(a) M = 2.44

Figure 7.- Lift, drag, and pitching-moment characteristics of model B.

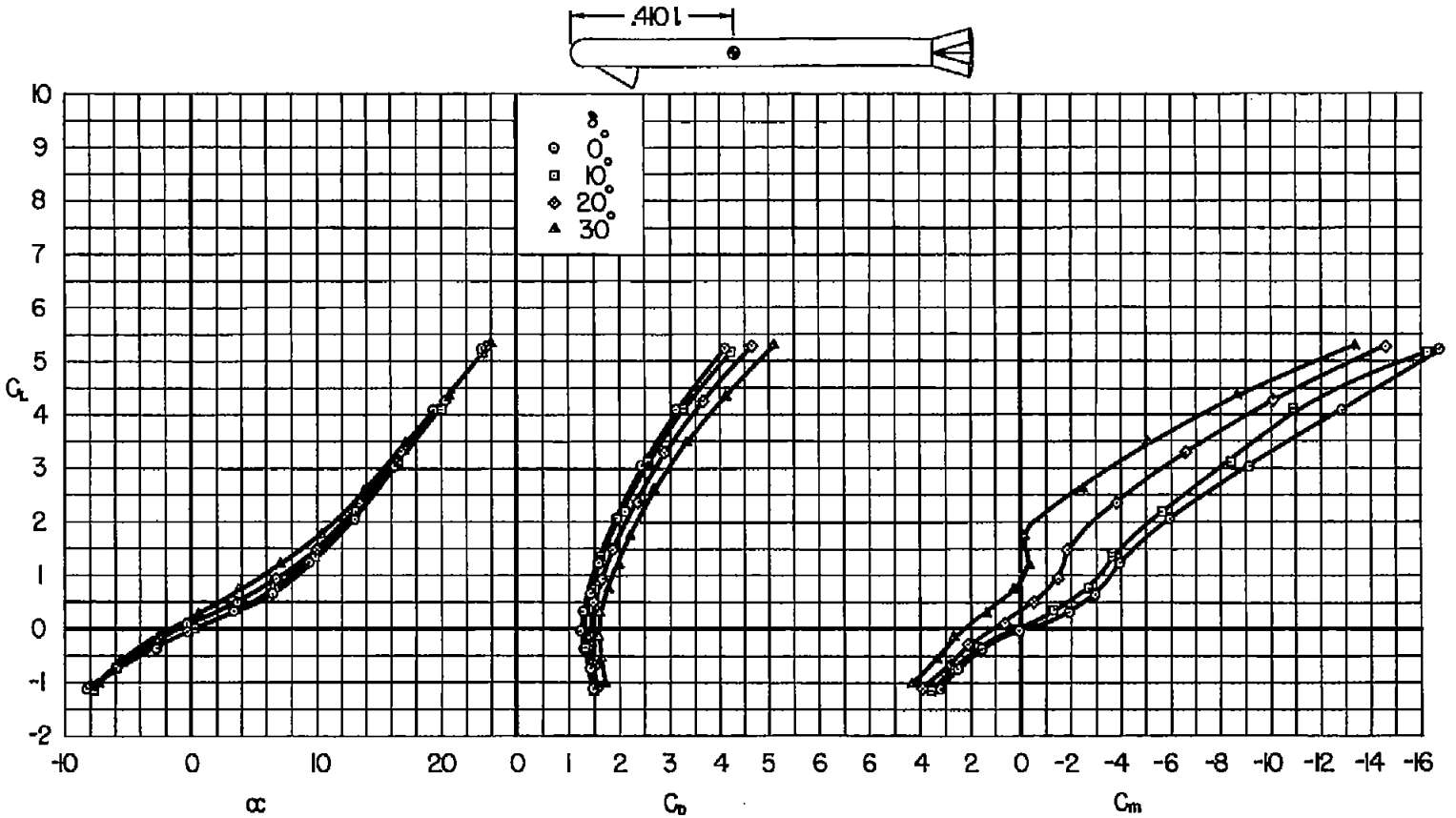

(b) M = 3.35

Figure 7.- Concluded.

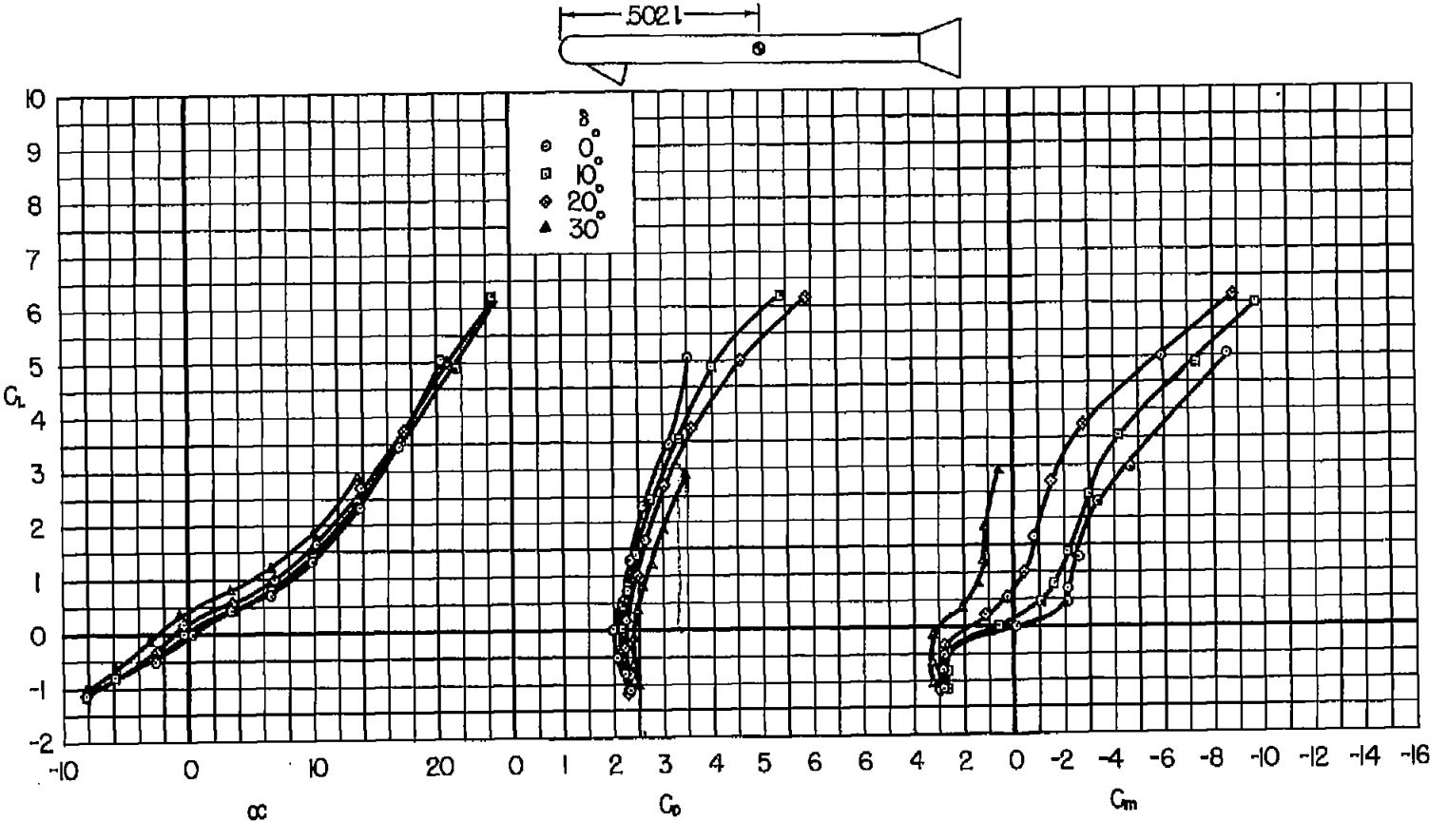

(a) M = 2.44

Figure 8.- Lift, drag, and pitching-moment characteristics of model C.

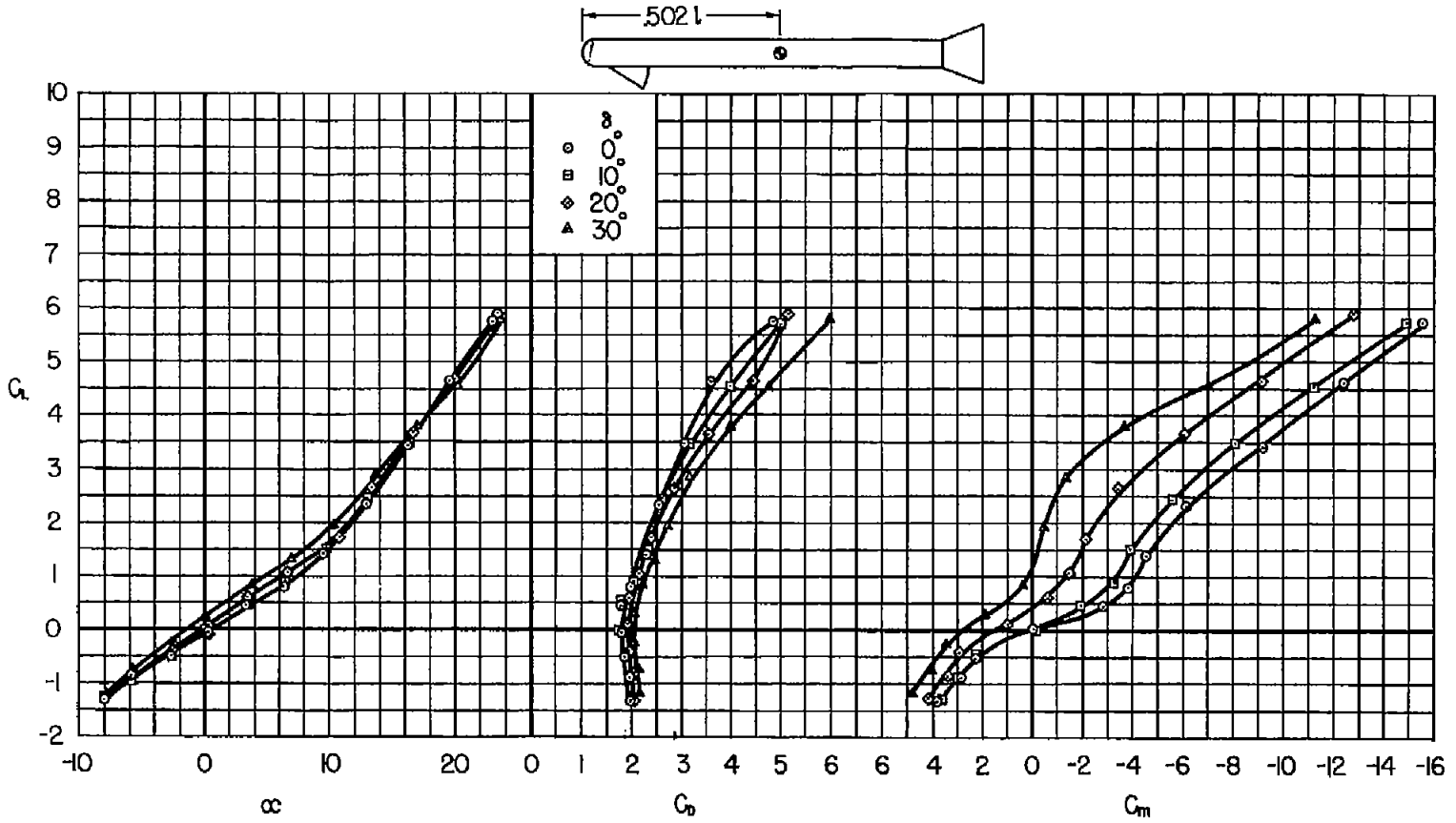

(b) M = 3.35

Figure 8.- Concluded.

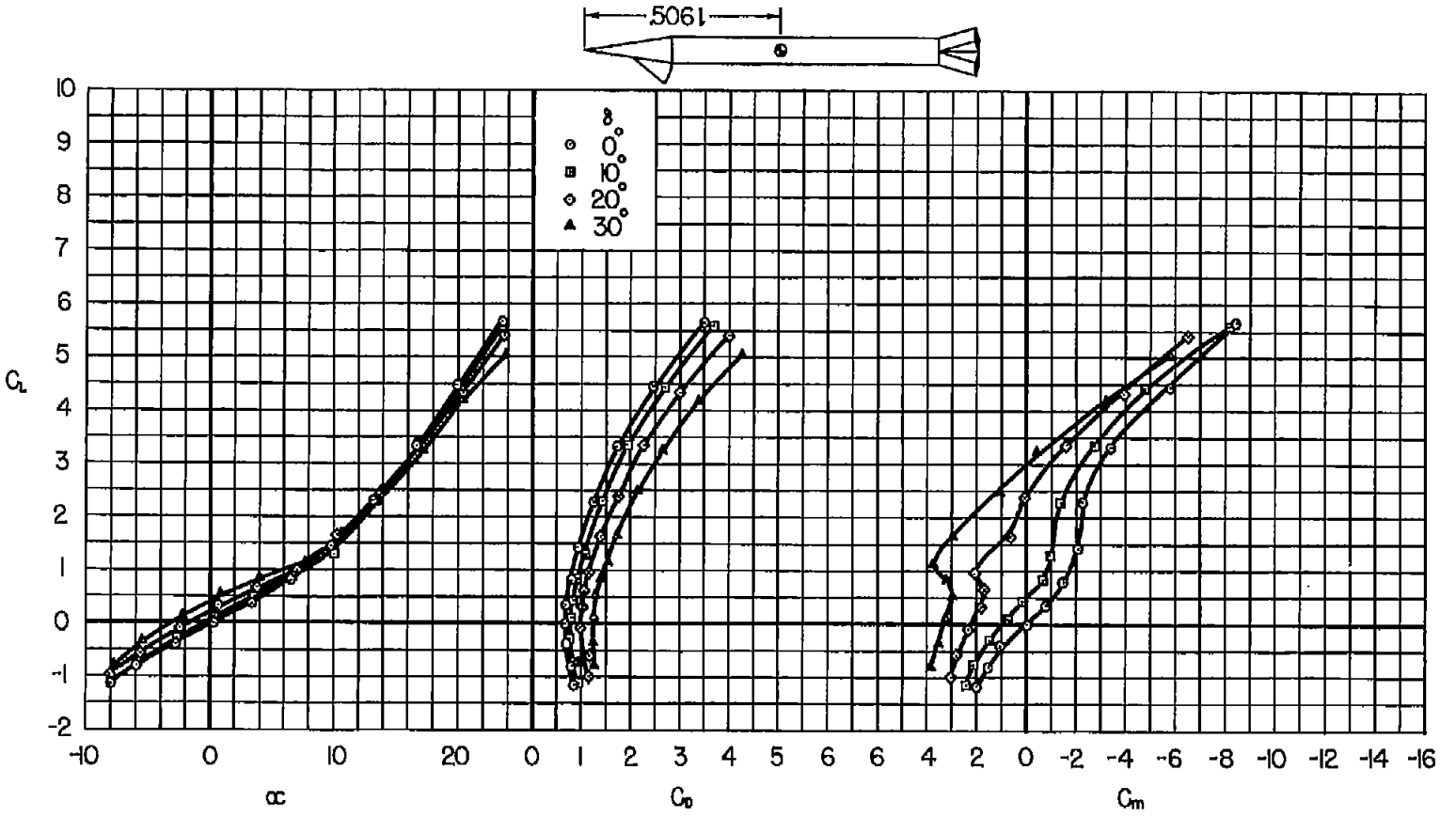

(a) M = 2.44

Figure 9.- Lift, drag, and pitching-moment characteristics of model D.

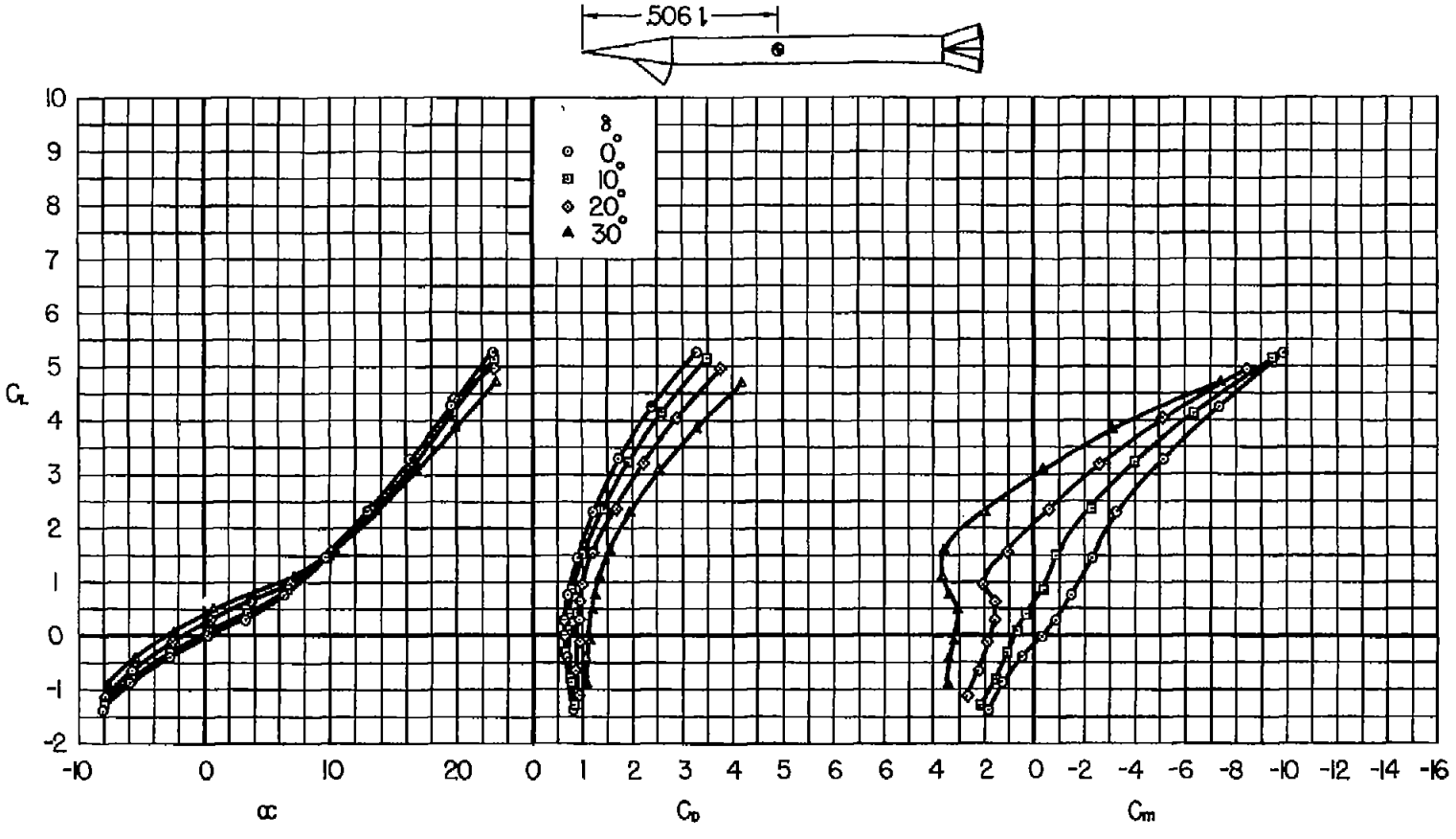

(b) M = 3.35

Figure 9.- Concluded.

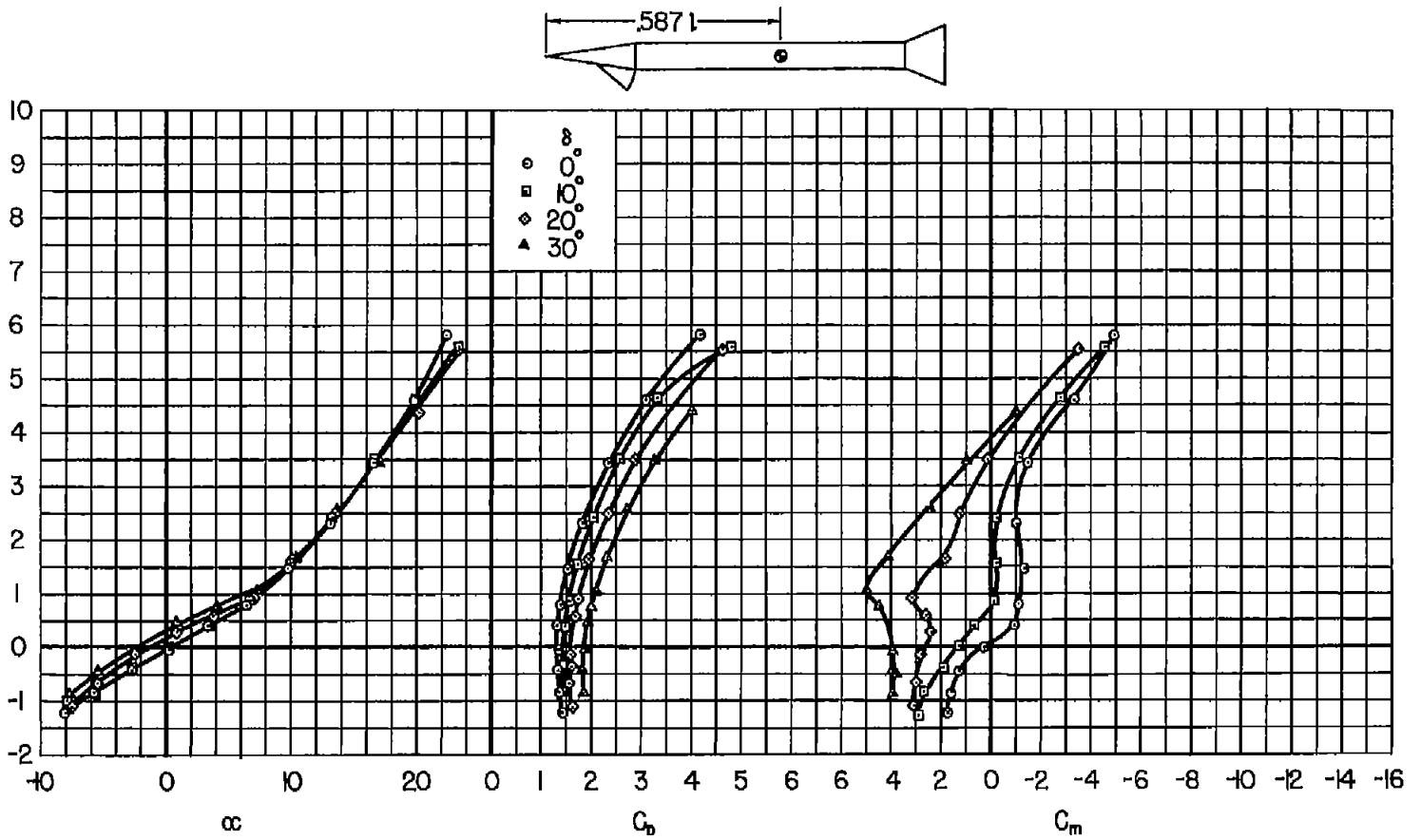

(a) M = 2.44

Figure 10.- Lift, drag, and pitching-moment characteristics of model E.

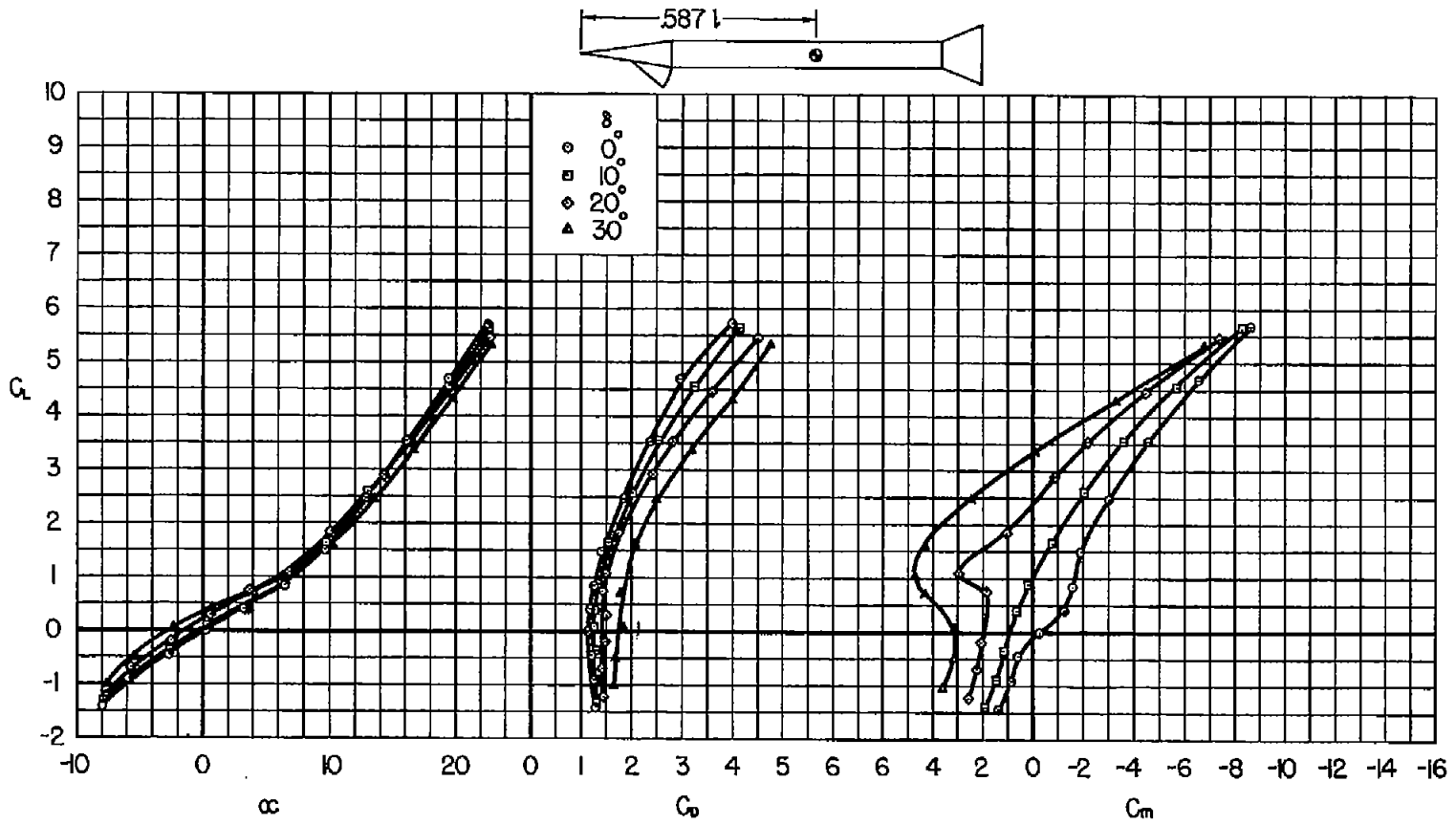

(b) M = 3.35

Figure 10.- Concluded.

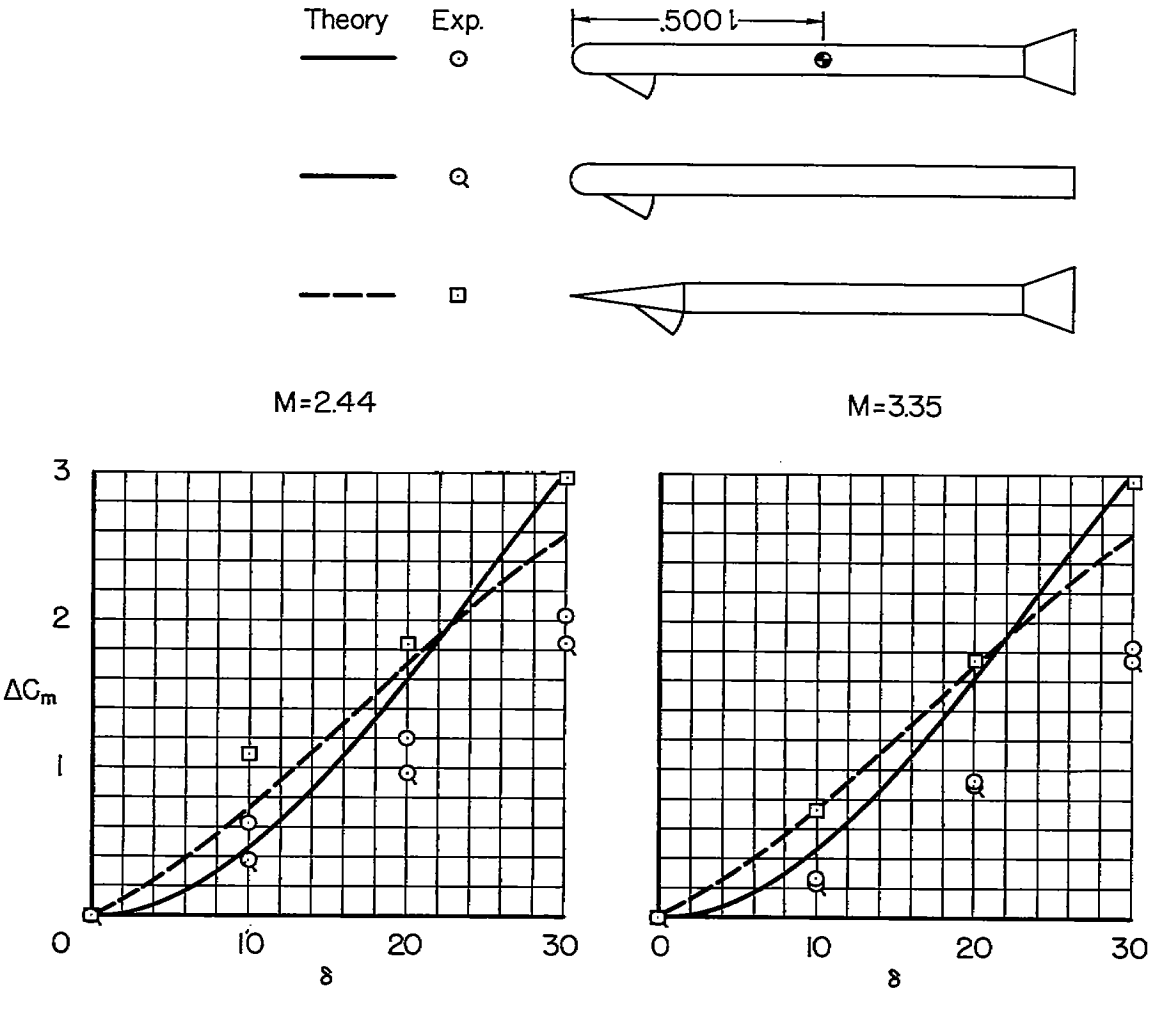

Figure 11.- Nose control effectiveness at $\alpha = 0^\circ$.

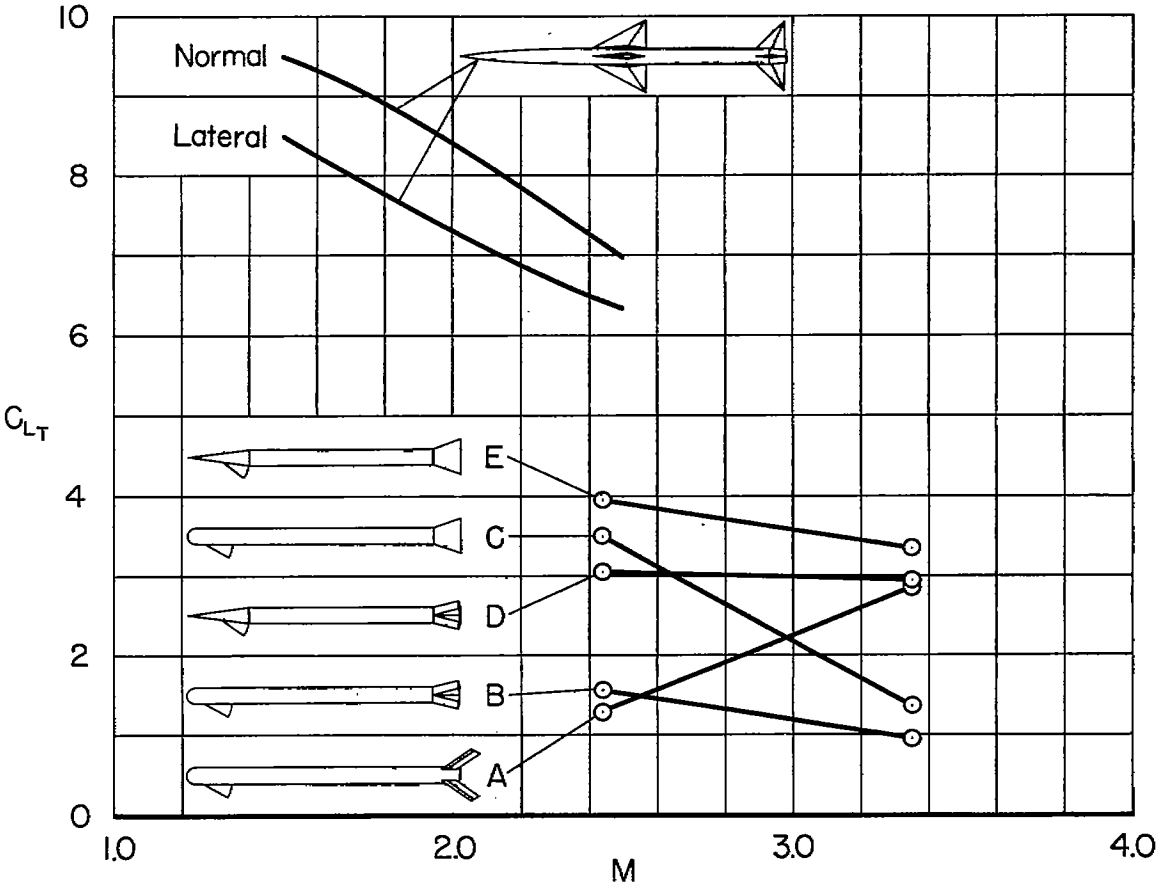

Figure 12.- Maximum trimmed lift coefficients for winged and wingless missiles.

[redacted]

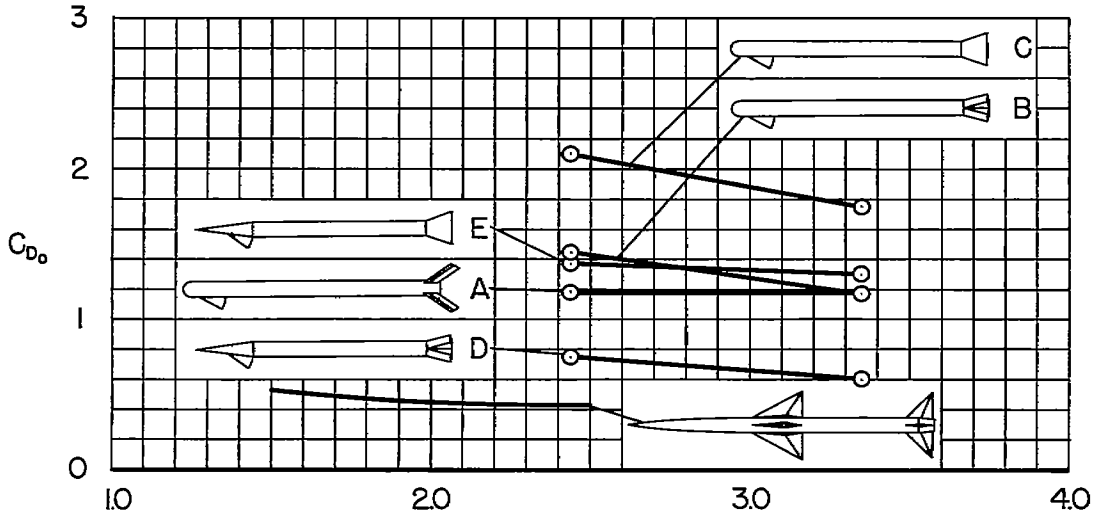

(a) Zero lift.

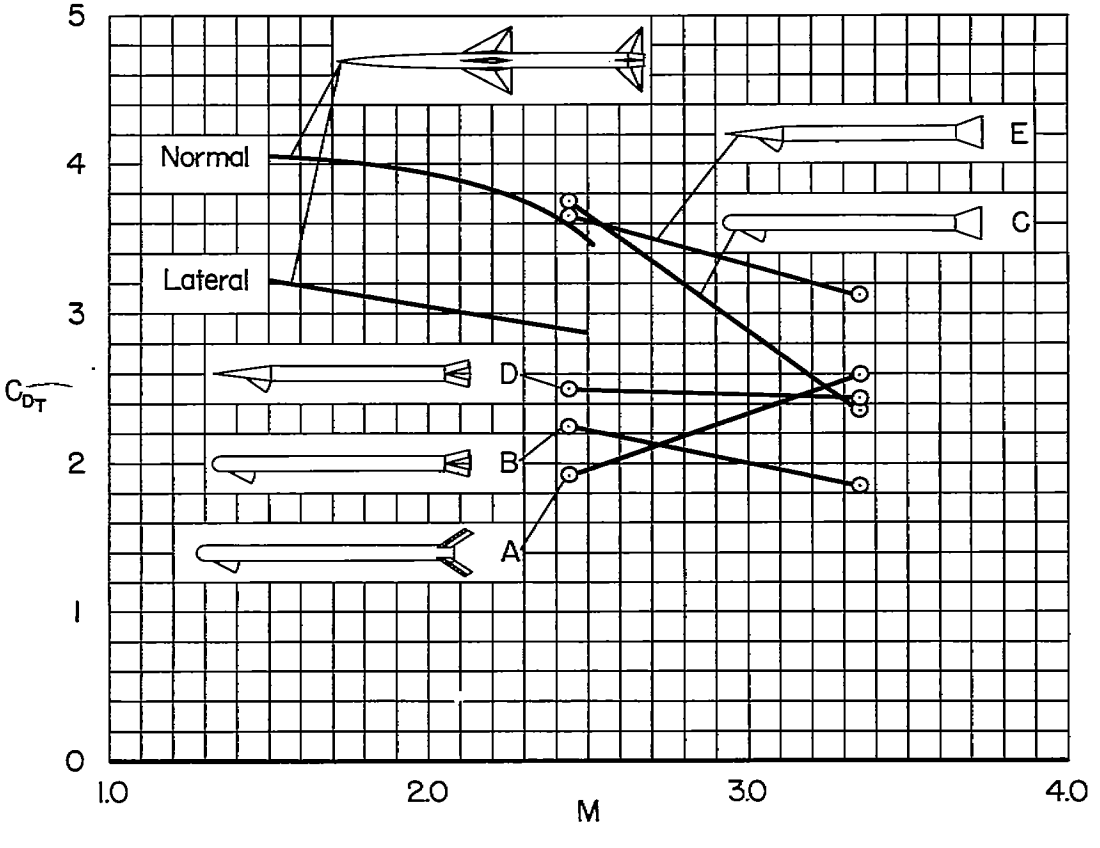

(b) Maximum trimmed lift.

Figure 13.- Drag coefficients for the winged and wingless missiles.

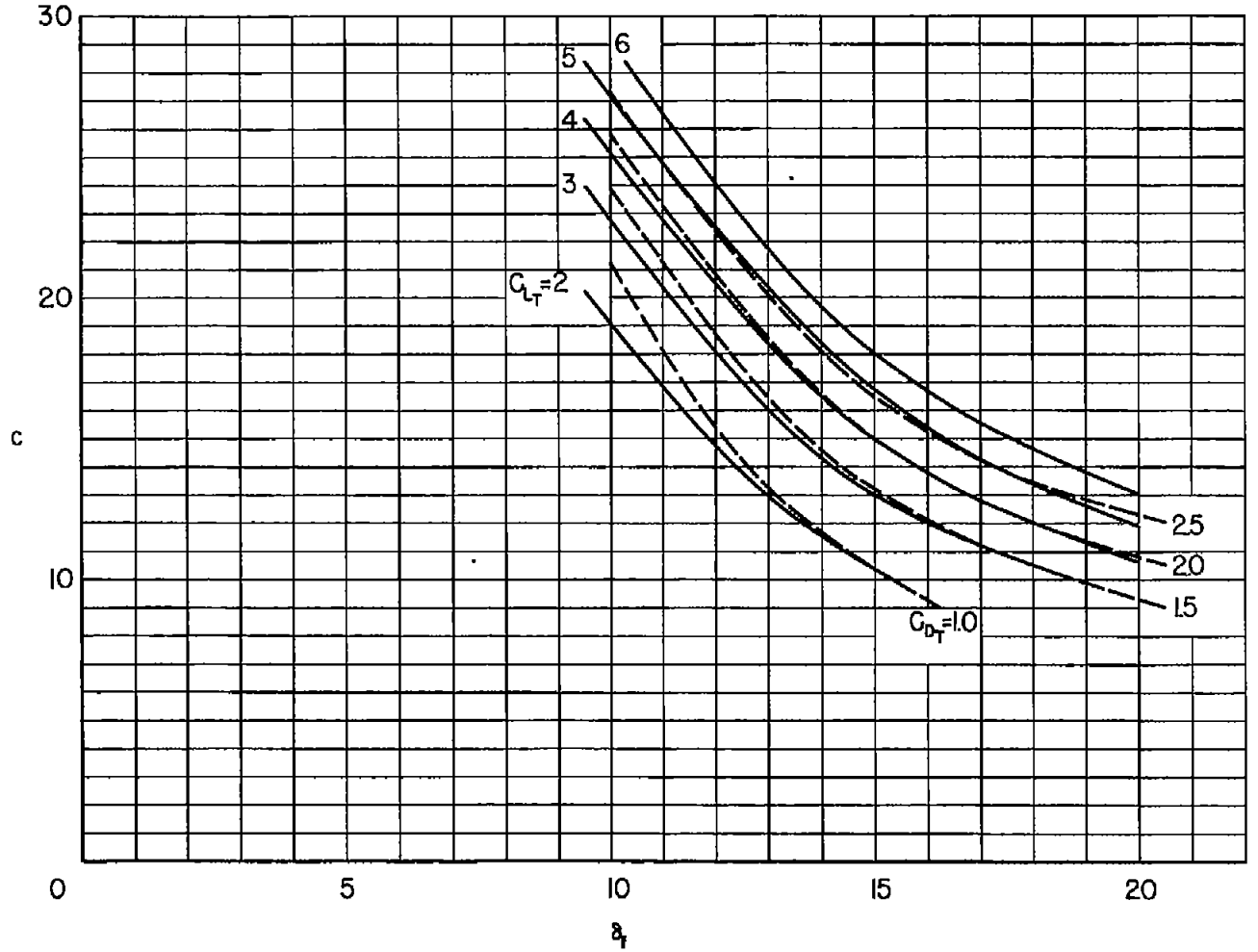

(a) Maximum trim lift and trim drag coefficients.

Figure 14.- The effect of variation in segment length and flare angle on maximum trim lift and trim drag coefficients and on the center-of-gravity location for a specified stability.

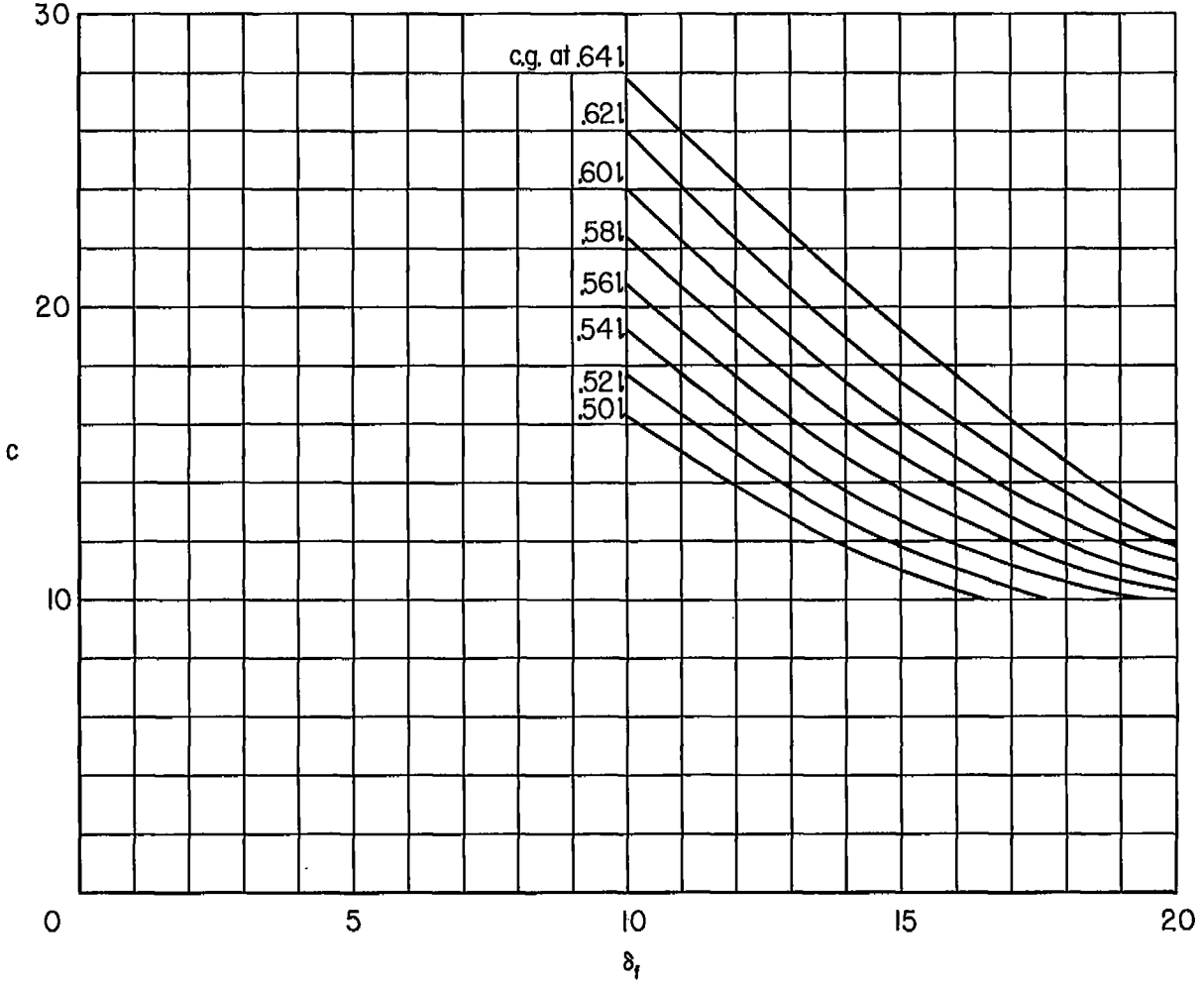

(b) Center-of-gravity location for a specified stability.

Figure 14.- Concluded.

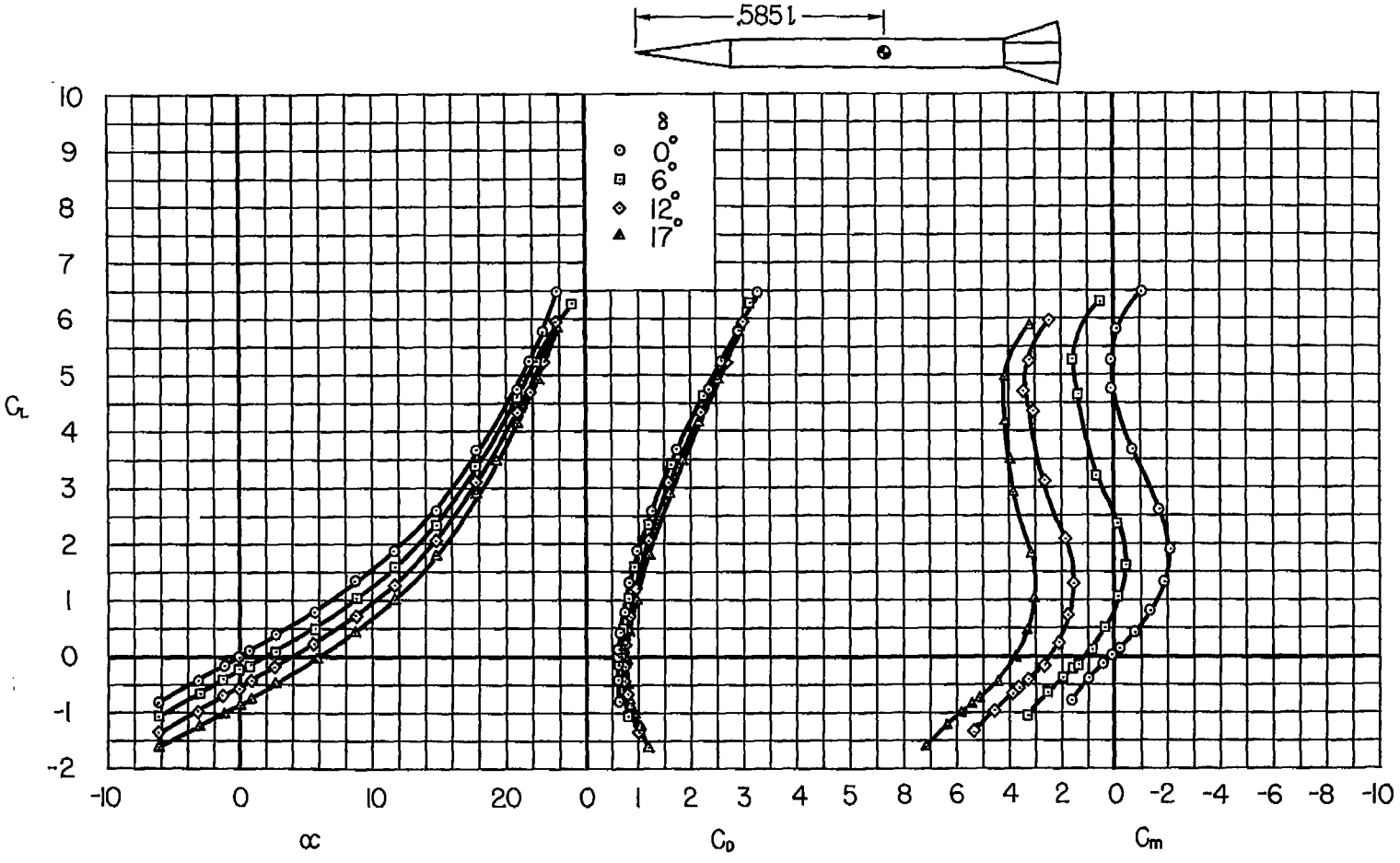

(a) M = 1.76

Figure 15.- Lift, drag, and pitching-moment characteristics of model G.

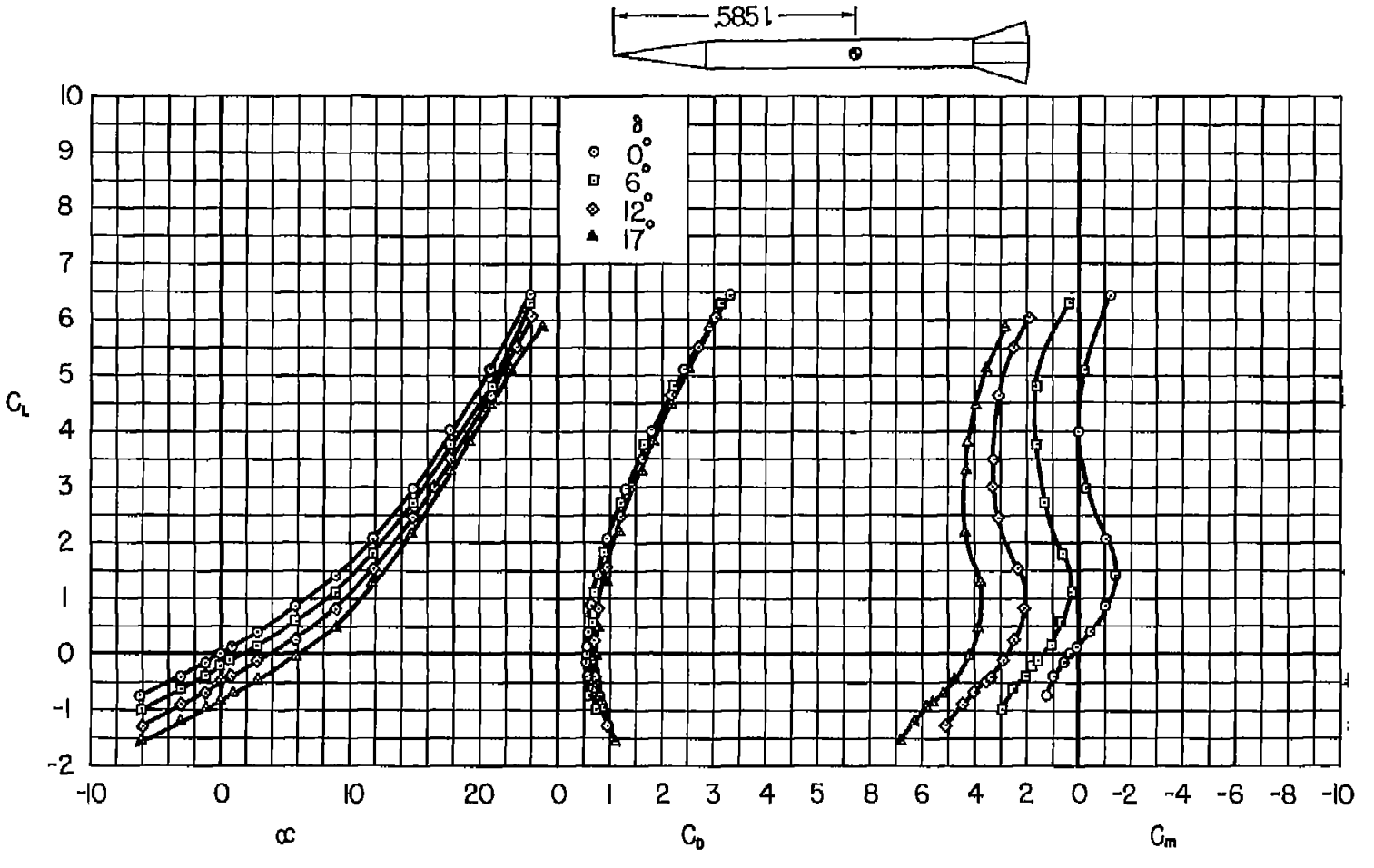

(b) M = 2.00

Figure 15.- Continued.

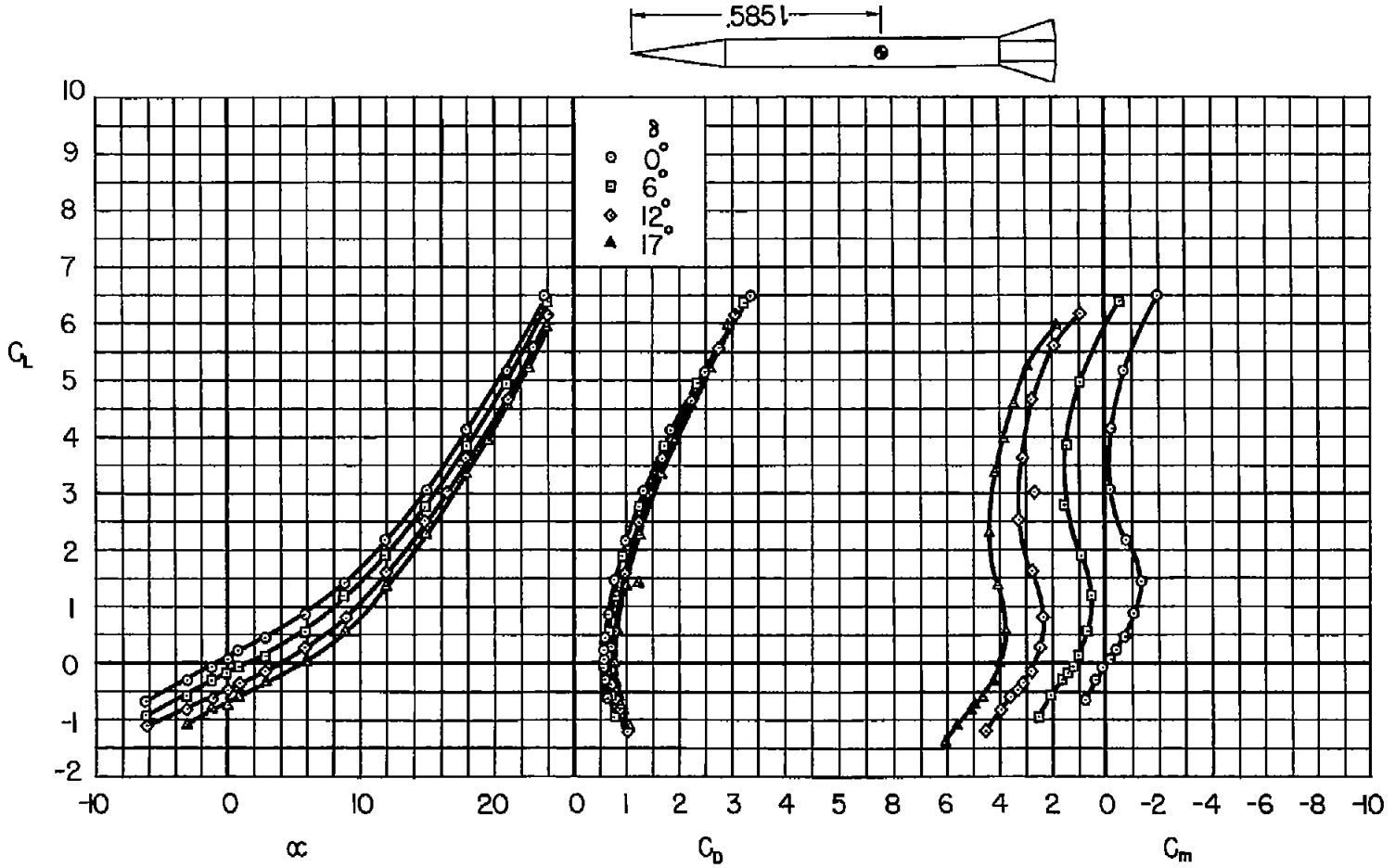

(c) M = 2.20

Figure 15.- Continued.

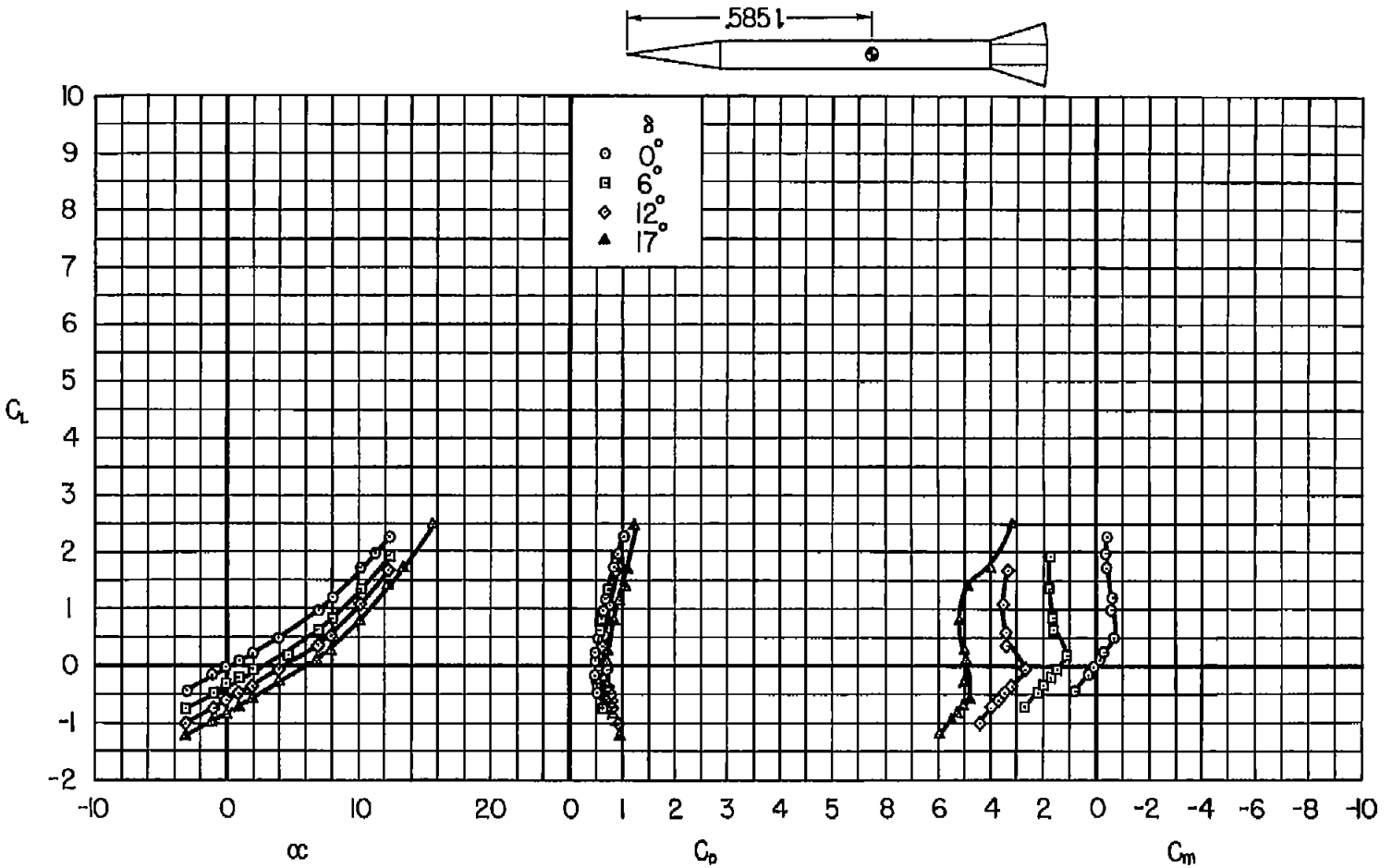

(d) M = 3.00

Figure 15.- Continued.

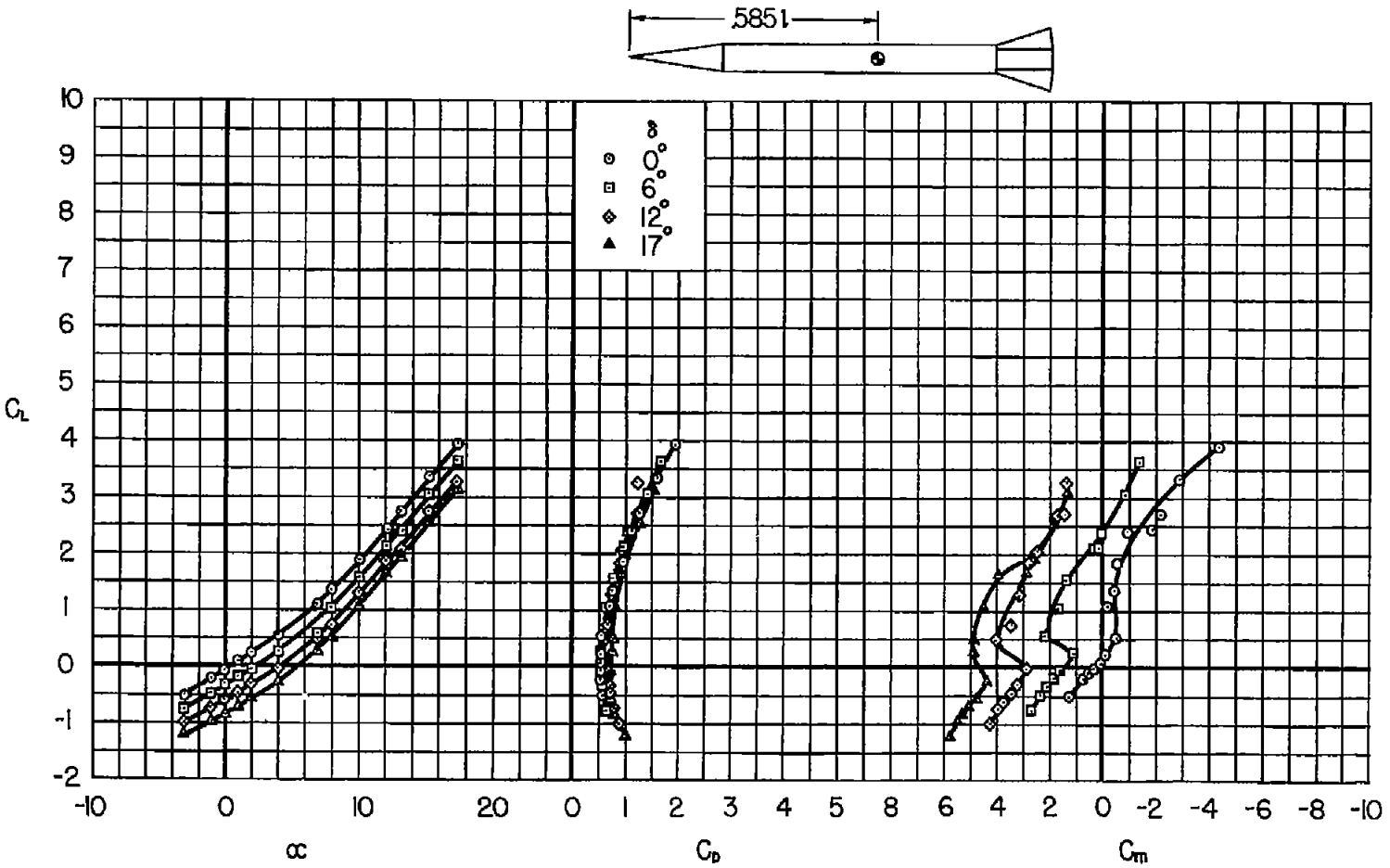

(e) M = 4.24

Figure 15.- Continued.

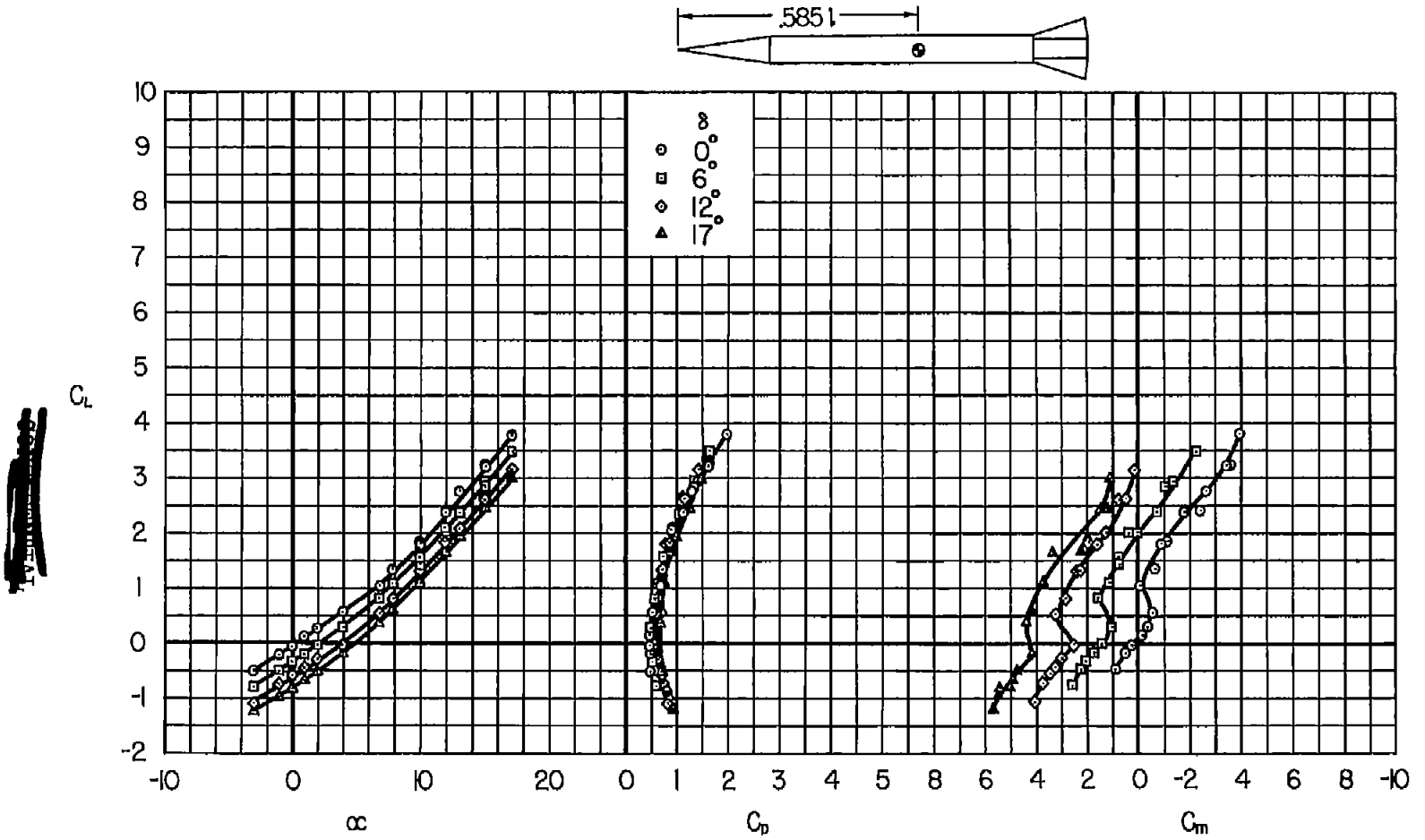

(f) M = 5.05

Figure 15.- Concluded.

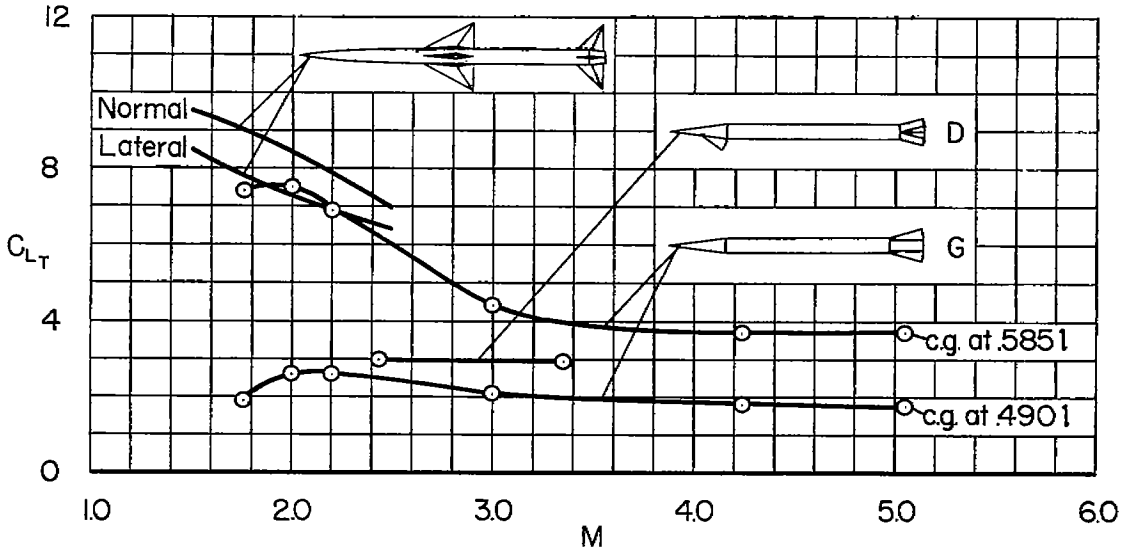

Figure 16.- Maximum trimmed lift coefficients for the winged missile and model G.

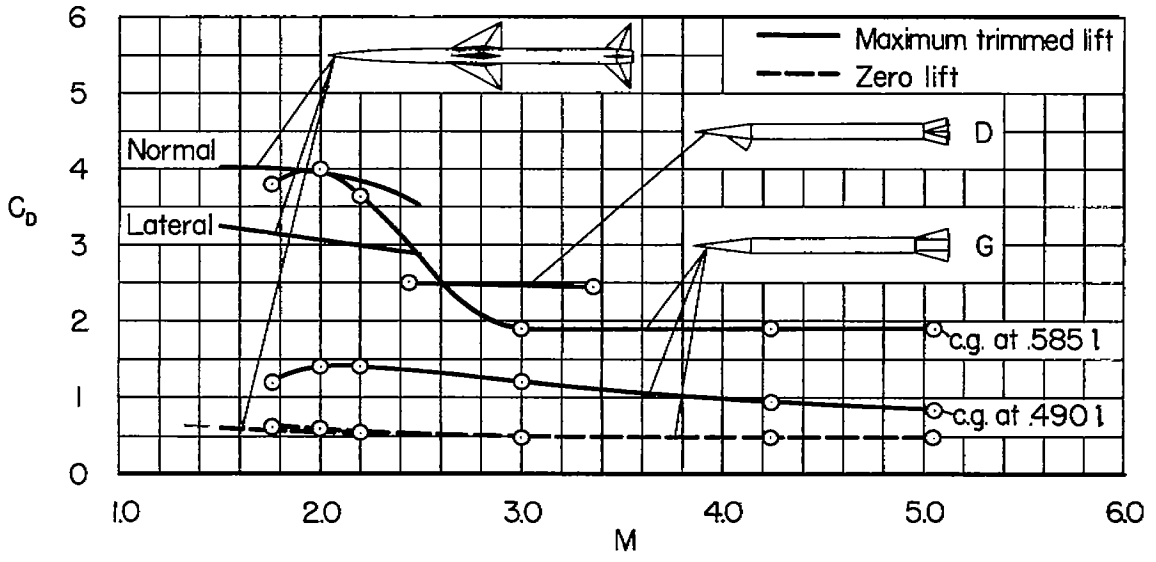

Figure 17.- Drag coefficients for the winged missile and model G.

[redacted]

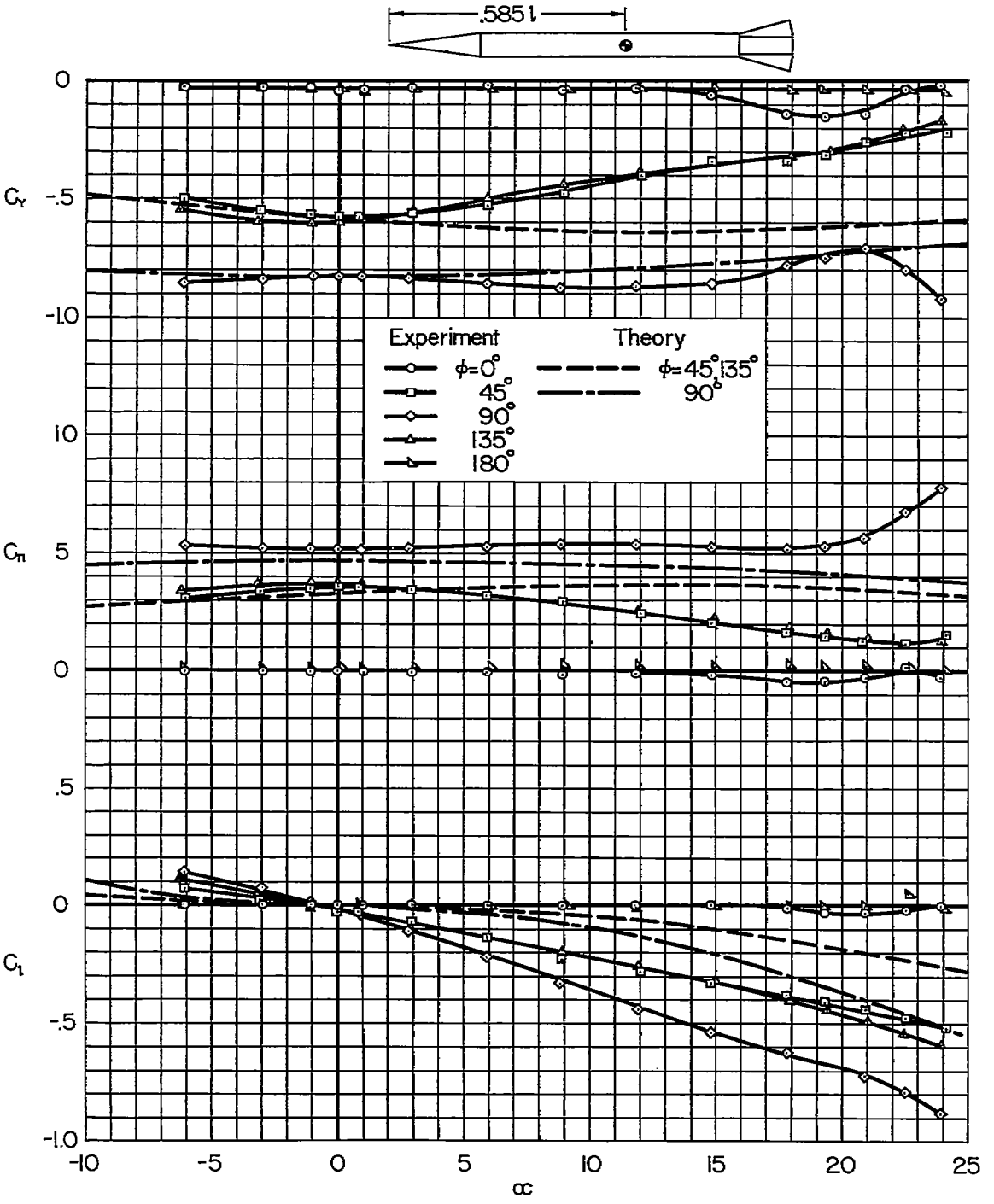

Figure 18.- Side-force, yawing-moment, and rolling-moment characteristics of model G at M = 2.00, δ = 17°.

[redacted]

UNCLASSIFIED

~~CONFIDENTIAL~~